Journal of Materials Chemistry B

ROYAL SOCIETY OF CHEMISTRY

REVIEW

View Article Online
View Journal | View Issue

Cite this: J. Mater. Chem. B, 2022, 10, 6571

Recent advances in protein-imprinted polymers: synthesis, applications and challenges

Yanting He[ab] and Zian Lin *[b]

Received 7th February 2022,
Accepted 14th April 2022

DOI: 10.1039/d2tb00273f

rsc.li/materials-b

The molecular imprinting technique (MIT), also described as the "lock to key" method, has been demonstrated as an effective tool for the creation of synthetic polymers with antibody-like sites to specifically recognize target molecules. To date, most successful molecular imprinting researches were limited to small molecules (<1500 Da); biomacromolecule (especially protein) imprinting remains a serious challenge due to their large size, chemical and structural complexity, and environmental instability. Nevertheless, protein imprinting has achieved some significant breakthroughs in imprinting methods and applications over the past decade. Some special protein-imprinted materials with outstanding properties have been developed and exhibited excellent potential in several advanced fields such as separation and purification, proteomics, biomarker detection, bioimaging and therapy. In this review, we critically and comprehensively surveyed the recent advances in protein imprinting, particularly emphasizing the significant progress in imprinting methods and highlighted applications. Finally, we summarize the major challenges remaining in protein imprinting and propose its development direction in the near future.

1. Introduction

Molecular recognition, which is the most extensive and subtle recognition mechanism in nature, plays a vital role in various biological processes such as DNA replication, cell division and differentiation, and immune responses in the immune system.[1] Because of the precise recognition properties, considerable attempts have been made to create synthetic recognition systems with high specificity and selectivity for certain molecules by utilizing biological macromolecules such as antibodies, receptors, enzymes and aptamers.[1–4] Despite their high selectivity and broad range of applications, these biomolecules always suffer from shortcomings such as low long-term stability and high manufacturing cost.[5,6] Therefore, developing stable, scalable, reusable and low-cost synthetic recognition systems remains an urgent need. To this end, molecular imprinting technique (MIT), which could obtain synthetic receptors with high selectivity toward target molecules, has attracted tremendous attention and has been proposed as an alternative for synthetic recognition systems.[7–9]

Molecular imprinting (MI) is a well-known technique that can fabricate synthetic polymers with tailor-made recognition sites toward certain template molecules or similar structured molecules. The idea of molecular imprinting originated from the natural recognition mechanism between antibodies and antigens, which was presented by Breinl and Haurowitz in 1930[10] and evolved with Mudd in 1932,[11] and was first proposed by Polyakov in 1931.[12] Based on Pauling's antibody theory[13] that antibody and antigen showed a specific three-dimensional space complementarity when contacting with each other, Dickey[14] reported in 1949 silica gels with specific affinity for dye molecules by preparing silica gels in the presence of template dyes. In 1972, Wulff and Sarhan[15] successfully prepared organic polymeric materials through a "covalent molecular imprinting" method, and the concept of molecular imprinting was really established. However, after that, molecular imprinting did not attract much attention. Until 1994, Mosach[16] introduced a "non-covalent molecular imprinting" method to synthesize crosslinked polymers in the presence of template molecules. Since then, the molecular imprinting technique began to develop rapidly and has achieved significant progress.

Generally, the synthetic polymers, defined as molecularly imprinted polymers (MIPs), are synthesized through three steps: (1) forming a complex between a target molecule (template) and functional monomers by self-assembly; (2) copolymerization of the complex and cross-linkers through various polymerization methods; (3) removal of the template using a rational washing protocol, as shown in Fig. 1.[17] The resulting MIPs show specific "memory" ability to recognize and bind template molecules, which is similar to the molecular recognition such as in

[a] School of Pharmacy, Bengbu Medical University, 2600 Donghai Avenue, Bengbu, Anhui, 233000, China
[b] Ministry of Education Key Laboratory of Analytical Science of Food Safety and Biology, Fujian Provincial Key Laboratory of Analysis and Detection Technology for Food Safety, College of Chemistry, Fuzhou University, Fuzhou, Fujian, 350108, China. E-mail: zianlin@fzu.edu.cn; Fax: +86-591-22866165

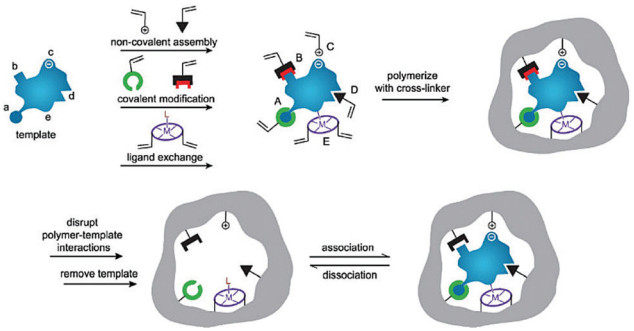

Fig. 1 Schematic illustration of the molecular imprinting process. Reprinted from ref. 17.

antibodies and enzymes in biological systems. Thus, MIPs have often been termed "synthetic/artificial/plastic antibodies" or "antibody mimics". However, compared to natural antibodies, MIPs possess several unique advantages.[18,19] In addition to the good affinity and selectivity comparable to antibodies, MIPs are more stable over time in harsh conditions such as under refrigeration or in acidity, resulting from long-term storage and have a wider range of applications. Besides, MIPs can be obtained through a simpler, faster, low-cost and even scalable method. Actually, the most attractive advantage of MIPs is to create synthetic receptors for target molecules whose natural binding partners and even the structures are unknown. Because of these features, MIPs have attracted strong interest among researchers and have been applied in various applications such as separation and purification,[20,21] target drug delivery,[22,23] chemical sensors,[24,25] proteomics,[26,27] artificial antibodies,[28,29] and medical diagnosis.[30,31]

To date, a wide range size of template molecules, including inorganic ions, organics, nucleic acids, peptides, proteins, viruses and whole cells have been extensively applied in the synthesis of various specific MIPs.[31,32] Among them, the majority of the publications and successful applications in molecular imprinting are aimed at the recognition and separation of small molecules. The development of MIPs for imprinting biological macromolecules, especially proteins, has been relatively slow.[33,34] Nevertheless, due to the tantalizing prospect of creating protein-imprinted polymers (PIPs) for biomedical and biodiagnostic applications,[28,29] much attention has been focused on the preparation of PIPs for specific and selective protein separation from complex biological samples. However, several obstacles pose great challenges to creating PIPs by traditional imprinting methods.[35,36] First of all, the large size made proteins difficult to diffuse into or out of the imprinted cavities, resulting in poor mass transfer and low protein desorption efficiency. To date, this issue has not been resolved but overcome to some extent by surface imprinting or epitope imprinting. Second, the structural and chemical complexity of proteins may cause non-specific binding and heterogeneous binding sites, subsequently affecting the binding behavior of PIPs. Besides, the protein's flexible structure and conformation, which are tightly related to the environmental changes, such as temperature, pH, ion strength and surfactant, may lead to the direct failure of the synthesis of PIPs.

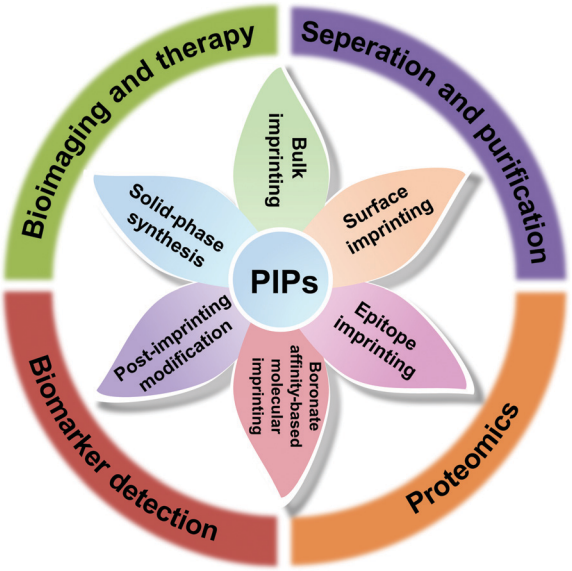

Fig. 2 Overview of the imprinting methods for PIPs and their related applications.

Despite the great challenges in protein imprinting, the past decade has witnessed substantial progress in the design and application of PIPs. In addition to the improvement and upgrading of traditional imprinting methods, several novel protein imprinting methods, including boronate affinity-based molecular imprinting, solid-phase synthesis and post-imprinting modification, have emerged and further spawned into several advanced applications, including separation and purification, proteomics, biomarker detection, bioimaging and therapy (Fig. 2). Although some reviews have focused on a certain protein imprinting method or application have been published,[37–40] a critical and comprehensive review is relatively scarce for summarizing the recent development of protein imprinting. In this review, we mainly focused on the recent developments in the imprinting strategies and highlighted applications for PIPs. Moreover, the challenges still existed in protein imprinting are discussed in detail and future prospects are also proposed.

2. Protein imprinting methods

Although molecular imprinting with proteins as the templates was first reported by Glad *et al.*[41] as early as 1985, the development of protein imprinting was still far behind small molecules. Due to the inherent properties of proteins, the traditional imprinting methods such as bulk imprinting, which were effective for small molecules, were not applicable to large proteins. However, after great efforts made over the past several decades, protein imprinting also has achieved significant progress. In addition to the improvement and upgrading of traditional imprinting methods, some advanced protein imprinting methods have emerged. Meanwhile, the successful examples of PIPs always integrated several imprinting methods together, rather than using only a single imprinting method. Up to now,

Table 1 Comparison of different imprinting methods for PIPs

Synthesis methods for PIPs	Merits	Drawbacks
Bulk imprinting	1. The most straight-forward method 2. High-density imprinting sites	1. Long binding equilibrium time caused by limited diffusibility 2. Non-specific adsorption for homologous peptides 3. Limited imprinting efficiency derived from the conformational changes and solubility of proteins 4. Binding sites will be destroyed by the mechanical crushing and grinding processes
Surface imprinting	1. Quick binding kinetics derived from the favourable accessibility of proteins in and out of the imprinted sites 2. Multiple advanced functionalities by using various nanomaterials as substrates	1. Limited binding capacity due to the relatively low amount of template proteins for imprinting
Epitope imprinting	1. The epitope peptides with simple structures could facilitate the immobilization and removal of templates; 2. Also, decrease the non-specific binding sites 3. Epitope peptides were more stable, more available and cost-effective	1. Ineffective when the amino acid sequence of protein is unknown 2. Suffer from limited accessibility to imprinted sites in the rebinding process
Boronate affinity-based molecular imprinting	1. The reversible boronate affinity could facilitate the immobilization and removal of glycosylation templates 2. Enhanced specificity for glycoproteins	1. Mostly used for glycoprotein imprinting
Solid-phase synthesis	1. Automated operation and short production time 2. High purity of nanoMIPs with high-affinity 3. Templates were reusable 4. More homogeneous binding sites and high specific affinity 5. High stability and good solubility of nanoMIPs 6. Advanced functionalities by introducing functional nanomaterials	1. Heterogeneous recognition sites from the variation of protein orientation 2. Low amount of templates immobilized on the solid support
Post-imprinting modification	1. Post-modification of the imprinted cavity 2. Introduce more functionalities by various chemical derivatization	1. Rational design of complex functional monomers 2. A tedious chemical synthesis procedure 3. The effect of chemical modifications on the rebinding process is unknown

protein imprinting methods can be mainly divided into traditional imprinting methods (bulk imprinting, surface imprinting and epitope imprinting) and emerging special imprinting methods (boronate affinity-based molecular imprinting, solid-phase synthesis and post-imprinting modification) (Fig. 2). In this section, we emphasized on reviewing the recent development of the protein imprinting methods and also discussed their merits and drawbacks (Table 1).

2.1. Traditional imprinting methods

2.1.1 Bulk imprinting. In a typical synthesis procedure of bulk imprinting, template molecules, functional monomers and crosslinkers are first mixed evenly to make them interact with each other, followed by bulk polymerization trigged by an initiator. After the templates are thoroughly removed by the optimal eluent, the resulting bulk polymer was transformed into small particles of appropriate sizes by mechanical crushing, grinding and sieving.[41–44] Obviously, the typical characteristic of bulk imprinting is to create MIPs with three-dimensional binding sites using a whole molecule as a template. Thus, bulk imprinting can also be called the "embedded" method and is the most straightforward protein imprinting method. Although bulk imprinting of small molecules is successful, the synthesis of MIPs by bulk imprinting with the entire protein as the template was hindered by some inherent barriers.[45–48] First, the limited diffusibility derived from the large size of proteins will cause long binding equilibrium time, poor regeneration and even the direct failure of PIPs.[45,46] Moreover, high-density sites imprinted from whole proteins could also provide affinity toward homologous peptides, which decreases the selectivity of PIPs. In addition, conformational changes in proteins and their solubility in the reaction media might greatly affect the imprinting efficiency of proteins.[47] Finally, the binding sites will be destroyed by the mechanical crushing and grinding processes, which reduced the rebinding ability of PIPs.[48]

Although the bulk imprinting of proteins is far behind that of small molecules, it is still the most simplest method for protein imprinting. In recent years, the traditional bulk imprinting of proteins has also shown some progress. Several special bulk imprinting forms have been reported to imprint proteins.[49–52] For instance, Boitard *et al.*[50] exploited a fast and simple polymerization method using a grafting process onto magnetic

nanoparticles to construct bovine serum albumin(BSA)-imprinted polymers by bulk imprinting. The resulting PIPs showed specific recognition and high adsorption capacity toward BSA. Notably, this imprinting process occurred in water media at room temperature, which might have the potential to imprint other proteins. This is the first example of a combination of bulk imprinting and grafting polymerization to synthesize PIPs. In addition, Tan *et al.*[52] prepared a novel type of polymer-assisted hierarchically porous PDA/$CaCO_3$ microparticles with a specific recognition ability toward lysozyme (Lyz). The authors called this method ''hierarchically bulk imprinting'', which could increase the binding capacity of PIPs by improving the accessibility of recognition sites to proteins. Although alternative imprinting methods have been highly recommended to solve, these drawbacks remained in the bulk imprinting of proteins in the past few years, the above recent progress indicates the possibility of improving this method by integrating the advantages of other imprinting methods.

2.1.2 Surface imprinting. To overcome the limitations of bulk imprinting, an alternative surface imprinting method was developed to synthesize MIPs in which the binding sites were exposed near or at the surface of the imprinted polymers. Compared with bulk imprinting, surface imprinting could provide favourable accessibility of proteins in and out of the imprinted sites, which leads to quick binding kinetics.[26,32,33,53–55] Thus, surface imprinting has become the most widely used and promising imprinting method regardless of the sizes of templates. Normally, surface-imprinted polymers were formed by synthesizing a thin polymer on the surface of a substrate with recognition ability toward proteins, followed by the construction of separation, sensor and diagnosis platforms.[31,56–58] However, unlike the whole proteins imprinted by bulk imprinting, the number of proteins imprinted by surface imprinting was relatively low, which leads to a decrease in binding sites. Meanwhile, the substrate used in surface imprinting often possesses a small surface-to-volume ratio. Therefore, traditional surface imprinted polymers always suffer from limited adsorption capacity toward proteins.[59] In recent years, nanomaterials, which possessed a high surface-to-volume ratio, and excellent physical and chemical properties, have been widely applied as the substrate for the surface imprinting of proteins.[37,60–62] The introduction of nanomaterials in surface imprinting could greatly increase the number of imprinted sites, then achieve better binding capacity. In addition, the introduction of some advanced nanomaterials also could endow PIPs with some special functionalities such as magnetic responsiveness and fluorescence properties, which have the potential to extend their wide applications.

Silica nanoparticles (NPs) are the most common substrates for surface imprinting of proteins mainly due to their chemical/mechanical stability, biocompatibility, controllable sizes, ease of preparation and functionalization. Fu *et al.*[63] synthesized core–shell surface-imprinted polymers of Lyz with modified silica NPs as the substrate. The silica NPs were pre-functionalized with double bonds and carboxylic acid groups using 3-aminopropyltrimethoxysilane and maleic anhydride. The double bonds could polymerize with crosslinkers and the carboxylic acid groups provided hydrogen bonds to interact with proteins. The resulted PIPs showed a high imprinting factor and large adsorption capacity toward Lyz. Then, our group[64] prepared highly monodisperse and uniform core–shell surface imprinted polymers of Lyz with vinyl modified silica NPs as the substrate. This method was simple and the resultant Lyz-MIP silica NPs could rebind Lyz from human serum, indicating good selectivity toward Lyz. Dopamine (DA), which could provide non-covalent interactions with proteins, is an ideal monomer for protein imprinting. Interestingly, it can self-polymerize under the basic conditions at room temperature. Based on this, our group[65] developed a facile method to synthesize polydopamine (PDA)-coated surface imprinted polymers of bovine hemoglobin (BHb) with non-modified silica NPs as the substrate. A thickness of only $\sim$5 nm of the surface imprinted PDA layer was obtained, which endowed the PIPs with rapid adsorption kinetics and high binding capacity. The successful application of the PIPs in deleting highly abundant BHb from cattle whole blood revealed their good potential in practical applications. Immobilized metal ion affinity chromatography (IMAC) is an effective method for the affinity separation and purification of proteins. Combining the IMAC and surface imprinting, Liu *et al.*[66] fabricated a new type of core–shell structured surface-imprinted polymers of porcine serum albumin (PSA) with Cu^{2+}-immobilized silica NPs as the substrate. The pre-modified Cu^{2+} could not only help to immobilize and remove the templates, but also provide recognition sites for rebinding PSA. The obtained PIPs displayed excellent selectivity and quick binding kinetics toward PSA. Hierarchical imprinting is a special surface imprinting strategy that creates imprinted polymers on the surface of the substrate and then sacrifices the substrate to expose the binding sites. Nematollahzadeh *et al.*[67] synthesized hierarchically imprinted polymers of human serum albumin (HSA) using wide pore silica particles as the substrate. Then, the silica matrix was further etched, which not only helped to remove the templates but also exposed the binding sites on the surface of imprinted polymers. The obtained PIPs possessed a high binding capacity toward HSA and could purify the functional HSA from blood serum, indicating their promising potential in biotechnology. Based on the inherent recognition mechanism of MIPs, Bhakta *et al.*[68] developed surface-imprinted silica NPs (AA_{HSA}) to rebind HSA and glucose oxidase (GOx) by hydrophobic, hydrophilic and hydrogen bonding interactions, which were similar to those between the antibody and antigen (Fig. 3). In this study, four organosilane monomers with amino acid-like residues were used to form antibody-like interactions with target proteins. Unfortunately, the AA_{HSA} showed a low adsorption capacity (5.9 mg g^{-1}) toward HSA. Recently, Zhang *et al.*[69] applied large pore silica as the substrate to successfully synthesize surface-imprinted polymers of BSA (MI-LPSPs). Similarly, two organosilane monomers were used to mimic antibody-like interactions to rebind BSA. Due to the introduction of large pore silica, the MI-LPSPs displayed a high adsorption capacity of 162.82 mg g^{-1} and fast adsorption kinetics toward BSA.

Magnetic NPs such as Fe_3O_4 NPs are the most often used solid supports for sample preparation due to their magnetic responsiveness, which could make the synthesis and separation

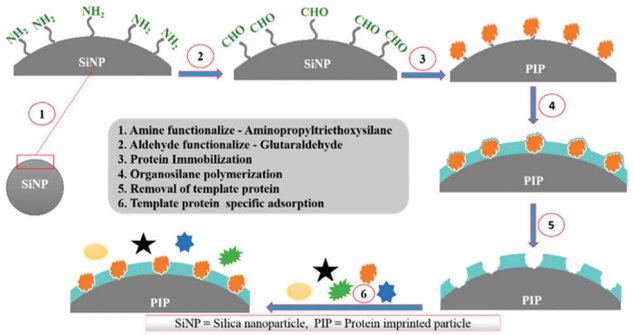

Fig. 3 The synthesis procedure and recognition process of artificial antibody sites. Reprinted from ref. 68.

procedure very convenient using an external magnet. Meanwhile, magnetic NPs are easy to prepare and post-functionalize, and also possess good biocompatibility and reusability. Thus, magnetic NPs were another attractive substrate for the surface imprinting of proteins.[37,40] Zhou *et al.*[70] simply prepared MIPs on the Fe_3O_4 NPs by self-polymerization of DA, and resultant magnetic PIPs showed good recognition abilities and high adsorption capacities toward target proteins. Gao *et al.*[71] successfully synthesized core–shell surface imprinted polymers with Fe_3O_4 NPs as the substrate. This imprinting method was demonstrated to be general for four proteins (BSA, BHb, Lyz, bovine pancreas ribonuclease A (RNase A)) with different isoelectric points. Among these proteins, the BHb–surface imprinted Fe_3O_4 NPs exhibited the best imprinting effect and highest adsorption capacity. The rebinding of BHb from the bovine blood demonstrated its good potential in practical applications. Based on their previous work,[68] Bhakta *et al.*[72] introduced the silica-coated Fe_2O_3 NPs as the substrate to construct HSA–surface imprinted polymers with antibody-like recognition sites toward target proteins. The magnetic cores endowed the PIPs with convenient separation and good reusability. Besides, ~88% of albumin could be extracted from human serum using these new HSA-MIPs, which revealed the great potential for practical use. Recently, combining the IMAC and self-polymerization of DA, zhou *et al.*[73] synthesized magnetic PDA-coated BSA-imprinted materials by a Ni^{2+}-BSA directional coordination strategy. Hollow Fe_3O_4@$mSiO_2$ microspheres served as the substrate. These well-designed PIPs possess high binding capacity, enhancing the imprinting factor and fast adsorption kinetics, and were successfully applied to rebind BSA from bovine serum samples. Generally, the major advantage of the introduction of magnetic NPs in the surface imprinting of proteins is the convenient separation procedure, which could extend the practical application of PIPs. In fact, their imprinting strategies did not have great differences from those of PIPs with silica NPs as the substrate.

Li *et al.*[74] synthesized surface imprinted nanowires with a general imprinting effect on several target proteins (albumin, hemoglobin, and cytochrome *c* (Cyt *c*)) for the first time. In a typical synthesis procedure, the *N*,*N*′-methylenebisacrylamide and acrylamide were polymerized on the nanoporous alumina membrane with the template proteins modified on their pore walls. After the alumina membrane was etched, the templates were removed and imprinting sites were exposed on the surface of the imprinted nanowires. Because of the large surface area of nanowires, these imprinted nanowires exhibited high binding capacity toward target proteins. Based on this study, Ouyang *et al.*[75] used the same method to synthesize surface-imprinted nanowires by self-polymerization of DA. Although the above two works exhibited a satisfactory imprinting effect, their synthesis procedures were tedious. To solve this problem, Chen *et al.*[76] directly fabricated BHb-imprinted PDA polymers on the surface of silica nanowires. Without the etching step, the surface-imprinted silica nanowires still displayed large binding capacity, quick binding kinetics, and outstanding reusability. Inspired by the excellent performance of nanowires, another one-dimensional substrate of carbon nanotubes was then widely applied to construct surface-imprinted polymers of proteins.[77–83] Zhang *et al.*[77] described the synthesis of BSA-imprinted polymers on multiwalled carbon nanotubes (MWCNTs) by the polymerization of acrylamide and *N*,*N*′-methylenebisacrylamide for the first time. Unfortunately, these BSA-surface imprinted MWCNTs showed low adsorption capacity and slow binding kinetics toward template proteins. Xu *et al.*[81] prepared Lyz-surface imprinted MWCNTs by self-polymerization of DA. Compared with other MIPs of Lyz, the highest binding capacity, excellent selectivity and good reproducibility were obtained in this study. To achieve high adsorption capacity and rapid adsorption kinetics, BSA–surface imprinted tubular carbon nanofibers (SIPTCFs) with self-driven properties were constructed by Yang *et al.*[82] Self-polymerization of DA occurred on the substrate of TCFs–COOH (Fig. 4). Because of the high specific surface area, cavity and porous tube wall, SIPTCFs could reach an excellent adsorption capacity of 541.99 mg g^{-1} within 1 h and showed high selectivity toward BSA. Based on this work, the same group[83] recently integrated the magnetic responsiveness with SIPTCFs to simplify the synthesis and separation procedure. The resultant surface imprinted magnetic tubular carbon nanofibers (SIPMTFs) still showed high capacity and good selectivity toward target proteins.

Compared with the above nanomaterials, graphene with a two-dimensional plane structure has a larger surface area, which is considered an ideal substrate to create surface-imprinted polymers with higher protein rebinding capacity.[84–87] For instance, graphene oxide (GO) nanosheets served as a novel substrate to yield

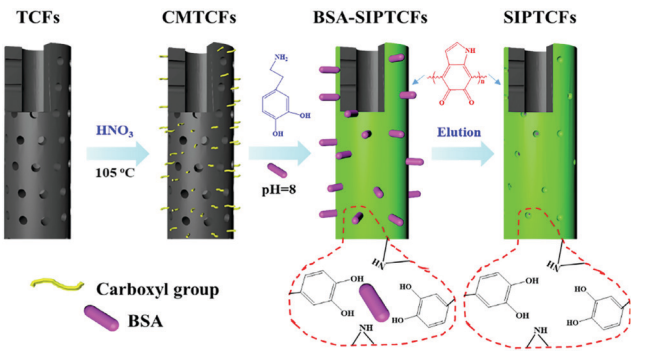

Fig. 4 Preparation of self-driven surface BSA imprinted tubular nanofibers. Reprinted from ref. 82.

BHb imprinted PDA@RGO.[84] The as-prepared BHb imprinted PDA@RGO presented an excellent binding capacity of 198 mg g^{-1} toward BHb and fast adsorption kinetics to achieve the 89% of the maximum capacity within 5 min. The imprinting factor of 4.95 was obtained, indicating a good selectivity of this imprinted material. This study demonstrated that the two-dimensional structure and large surface area of GO could provide MIPs with enhanced binding capacity and more accessible recognition sites for target proteins. However, this type of graphene-based MIPs is tedious in the synthesis and separation processes. To this end, Fe_3O_4–graphene composites were then utilized as the substrate for the surface imprinting of proteins.[85] Fe_3O_4–GO composites were first obtained by co-precipitation method and then used as the supporting substrate to fabricate Fe_3O_4–graphene PDA-based 2D MIPs with DA as the monomers and BSA as the templates. Benefiting from the large surface area of GO, the resulting PIPs displayed a high binding capacity of 117.1 mg g^{-1} and good selectivity for BSA and could be successfully applied in bovine blood samples.

Semiconductor fluorescent nanomaterials often termed ''quantum dots (QDs)'' are featured by their outstanding optical and electrical properties. Optical biosensors with increased stability, sensitivity and selective fluorescence response could be constructed by integrated surface imprinted polymers with QDs.[60,61,88,89] For the first time, Tang *et al.*[90] demonstrated the validity of the combination of CdS QDs and MIT to synthesize BSA–surface imprinted polymers for target protein recognition. The CdS QDs not only provided large specific surface areas, which were beneficial to high binding capacity but also were responsive to the binding with a template, which led to the quenching of the photoluminescence emission of CdS QDs. Zhang *et al.*[91] then successfully prepared fluorescent Cyt *c*-imprinted CdTe QDs composites with tetraethoxysilane as the crosslinker and 3-aminopropyltriethoxysilane as the functional monomer. CdTe QDs were stabilized by 3-mercaptopropionic acid (MPA) and functionalized with carboxylic acid groups at the same time. The luminescence of CdTe QDs was quenched when Cyt *c* was rebound by the MIP-coated CdTe QDs. A linear range was from 0.97 μM to 24 μM, and the detection limit was 0.41 μM when using MIP-coated CdTe QDs to recognize Cyt *c*. The same imprinting method was further utilized to develop MIP-coated CdTe QDs for three template proteins (Lyz, Cyt *c*, and methylated BSA).[92] However, the difference was that the denatured BSA-stabilized CdTe QDs were used, and also could provide recognition sites for target proteins. To enhance the binding capacity and accessibility of imprinting sites, MWCNT-QDs were later introduced to synthesize BSA–surface imprinted fluorescent polymers.[93] Benefiting from the large surface area of MWCNTs, the resultant BMIP-coated MWCNT-QDs exhibited a fast binding response time of 25 min and high binding selectivity toward BSA. The linear range was 5.0×10^{-7}–35.0×10^{-7} M, and the detection limit was 80 nM.

Although QDs have been successfully applied in PIPs, the toxicity and chemical instability greatly limit their wide applications. In contrast, upconversion nanoparticles (UCNPs) are more advantageous fluorescent materials due to their low toxicity, low photo-bleaching, long lifetimes, and lack of autofluorescence. Guo *et al.*[94] demonstrated the feasibility of using UCNPs as the fluorescent substrate to construct the protein surface imprinted fluorescent materials. A sol–gel reaction occurred around Cyt *c* (template protein) on the surface of UCNPs. The obtained UCNPs@MIP exhibited strong fluorescence changes for the rebinding with Cyt *c* and the imprinting factor was 3.19, indicating a good selectivity of UCNPs@MIP. Encouraged by this study, the same group combined MIT with UCNPs and metal-organic frameworks (MOFs) to fabricate UCNPs/MOFs/MIP composites.[95] In this study, BHb was chosen as the template, which has a metal coordination interaction with the Cu^{2+} in MOFs (HKUST-1). MOFs are attractive porous framework materials in various applications because of their fascinating properties including high specific surface area, tunable size and post-functionalization. Thus, the introduction of MOFs could increase the number of recognition sites and facilitate the mass transfer of UCNPs/MOFs/MIP toward target proteins. Meanwhile, a functional monomer of *N*-isopropyl acrylamide (NIPAAM) was used, resulting in the swelling and shrinking when the temperature changed. Finally, UCNPs/MOFs/MIP exhibited strong fluorescence changes toward the rebinding with BHb and achieved a high adsorption capacity of 167.6 mg g^{-1}.

Furthermore, MOFs have also been introduced as a single substrate to synthesize surface-imprinted polymers of proteins. Taking advantage of MOFs including high specific surface area and porous structure, this type of PIPs always showed outstanding binding capacity and kinetics. Li *et al.*[96] applied MOF-74(Ni) as the substrate to form surface-imprinted polymers of Lyz *via* the self-polymerization of DA. The MOF-74(Ni) not only provided a high specific surface area of 150.0 m^2 g^{-1}, but also facilitated the immobilization and rebinding of Lyz through the metal chelation of Ni^{2+}. A thickness of 10 nm for the imprinted layers was obtained, which enabled a fast binding kinetic of 10 min. Encouragingly, the resulting MOF@PDA-MIP achieved a significant binding capacity of 313.5 mg g^{-1} and imprinting factor of 7.8, demonstrating that MOFs are promising materials for the surface imprinting of proteins. Inspired by this study, Qian *et al.*[97] utilized MOFs/carbon nanoparticle (CN) composites (CN@UIO-66) as the substrate to construct the protein surface imprinted polymers. Interestingly, the resulting CN@UIO-66@MIPs possessed a high specific surface area of 551.4 m^2 g^{-1}, which led to an extremely high binding capacity (815 mg g^{-1}) toward Cyt *c*. Meanwhile, a high imprinting factor of 6.1 and rapid adsorption kinetics of 40 min were obtained.

As discussed above, compared with bulk imprinting, surface imprinting has become an advantageous method for creating PIPs due to their favourable accessibility to target proteins. Just as a coin has two sides, surface imprinting for proteins easily suffers from low binding capacity because of the decrease in recognition sites. Nanomaterials, featured by their high specific surface area, could be introduced as the imprinting substrate to solve this problem. Thus far, various nanomaterials, including silica NPs, magnetic NPs, MWCNTs, graphene, QDs, UCNPs and MOFs, have been applied as the substrate to fabricate

protein–surface imprinted polymers. It should be noted that, in addition to the improvement of binding performance, the introduction of nanomaterials could endow protein–surface imprinted polymers with some special functionalities such as magnetic responsiveness and fluorescence properties, which have the potential to extend their wide applications. With the rapid upgrade of nanomaterials, more protein surface imprinted polymers with excellent adsorption performance and advanced functionalities will be developed in the future.

2.1.3 Epitope imprinting. Although surface imprinting could solve the limitation of accessibility of imprinting sites remaining in bulk imprinting to some extent, using the whole protein as a template still hinders the development of protein imprinting due to the inherent properties of proteins. To this end, Rachkov *et al.*[98] developed an "epitope imprinting" method to successfully synthesize PIPs by using a tetrapeptide (YPLG) as the template. The resultant PIPs could rebind peptides and proteins based on the recognition mechanism between the antibody and antigen. In the typical epitope imprinting of proteins (Fig. 5), a polypeptide exposed on the surface of proteins was employed as the temple, which led to many advantages in comparison with the use of whole protein. First, the decrease in template complexity could not only facilitate the immobilization and removal of templates but also decrease the non-specific binding sites derived from multi-functionalities of proteins. Second, polypeptides are more stable against the environmental changes and more compatible with aprotic organic solvents during the synthesis process, which could avoid the problem of conformational change and insolubility of proteins. In addition, a peptide can be chemically synthesized, so it is more available and cost-effective. Obviously, epitope imprinting seems to address all the obstacles in protein imprinting derived from the inherent properties of proteins and has been a promising strategy for protein imprinting.[28,38,39,48,99,100] Despite the advantages of epitope imprinting in the synthesis procedure, it can not avoid the problem of accessibility to imprinted sites in the rebinding process. Therefore, epitope imprinting is more attractive for surface imprinting rather than bulk imprinting.

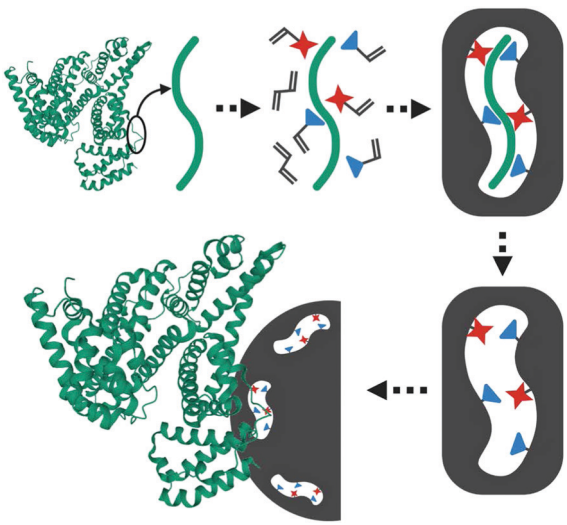

Fig. 5 Rationale of the epitope imprinting concept. Reprinted from ref. 99.

Nishino *et al.*[101] developed a general method to create surface-imprinted polymers toward three proteins (Cyt *c*, Lyz and alcohol dehydrogenase (ADH)) by epitope imprinting. Unique epitope peptides (nine amino acid sequences) exposed on the surface of three proteins were used as the templates. After the epitope peptides were immobilized on the pretreated glass or silicon surface, the polymers were formed by free radical polymerization. Then, the imprinted sites were exposed by the etching of the glass or silicon to yield the protein-imprinted polymer film. Yang *et al.*[102] synthesized transferrin (TRF) epitope imprinted polyethersulfone (PES) beads by self-assembly polymerization around the epitope template of the N-terminal sequence (MRLAVGALL). The transferrin epitope imprinted particles showed excellent binding capacity and selectivity toward transferrin epitope and transferrin, and were successfully applied in a real sample of human plasma. Then, the same group[103] tried to develop a multiepitope imprinting strategy to synthesize multiepitope imprinted particles using the same PES self-assembly method. Three epitope peptides of proteins (HSA, TRF, and immunoglobulin G (IgG)) were selected as the templates. The resulting multiepitope imprinted particles could simultaneously capture three proteins from the complex human plasma, indicating the promising potential of this multiepitope imprinting strategy in practical applications. Zhao *et al.*[104] synthesized magnetic surface epitope-imprinted polymers with a core–shell structure (Fe_3O_4@EMIPs) for the separation of BSA by combining epitope imprinting, surface imprinting, and Fe_3O_4 NPs. The introduction of Fe_3O_4 NPs made the synthesis and separation procedure more convenient. The as-prepared Fe_3O_4@EMIPs showed high selectivity toward BSA from bovine blood, indicating their good potential in real use. Li *et al.*[105] applied His-tag-anchored epitope from HSA as a template to provide a new oriented surface imprinting method. The surface imprinting occurred on the Fe_3O_4@SiO_2@IDA@Ni^{2+} substrate. The introduction of strong metal coordination between Ni^{2+} and His-tag-anchored epitope could make the immobilization and removal of templates more convenient. After optimizing the utilization efficiency of templates and thickness of the imprinted layer, the obtained epitope-oriented surface-imprinted nanoparticles exhibited specific recognition ability toward HSA. Based on this study, the same group[106] then prepared epitope-oriented surface-imprinted nanoparticles using His-tag (HHHHHH) as the template and were further applied to purify His-tagged proteins. In this example, the IMAC could not only help to immobilize and remove templates but also provide affinity sites for rebinding His-tagged proteins. Due to the high selectivity of MIT, the authors called this method "Epitope imprinting enhanced IMAC (EI-IMAC)". Qin *et al.*[107] created epitope-imprinted polymers with magnetic carbon nanotubes (MCNTs) as the substrate, epitope peptide (AYLKKATNE) derived from Cyt *c* as the template (Fig. 6). MCNTs@EMIP was fabricated by free radical polymerization using ethylene glycol dimethacrylate

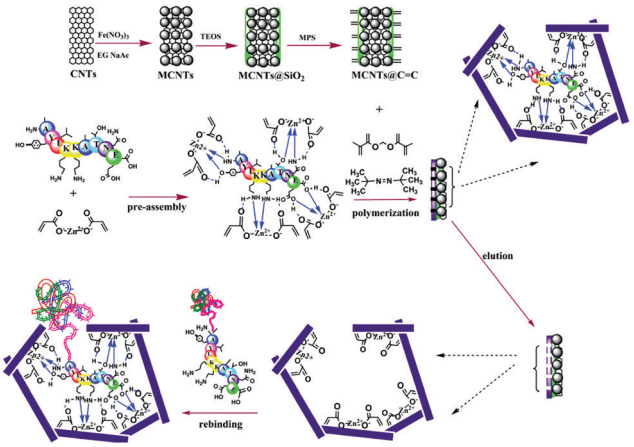

Fig. 6 Synthesis protocol of MCNTs@EMIP *via* surface imprinting and epitope imprinting. Reprinted from ref. 107.

(EGDMA) as a cross-linker and zinc acrylate as a functional monomer. The hydroxyl and amino groups of the epitope could form a five-membered ring with the Zn^{2+}. Together with the large surface area of CNTs, these PIPs achieved an extremely high binding capacity of 780.0 mg g^{-1} and an imprinting factor of 11.7. The outstanding binding performance showed the successful separation of Cyt *c* from a real bovine blood sample, indicating the excellent selectivity of MCNTs@EMIP and promising potential in real use. Li *et al.*[108] synthesized thermo-sensitive epitope surface imprinted polymers by combining carbon dots (CDs) and SiO_2. Double templates of epitope peptides derived from C- and N-terminals of Cyt *c* were used. The resulted CDs/SiO_2/MIP exhibited fluorescence quenching when rebinding with the target protein of Cyt *c*. Then, a linear range of 0.1–40 μM and a detection limit of 89 nM were obtained. Meanwhile, the temperature-sensitive monomer endowed the CDs/SiO_2/MIP with swelling and shrinking capabilities with temperature changes.

Generally, epitope imprinting is the most potent protein imprinting method because they are based on the recognition mechanism between antibody and antigen is consistent with MIT, which is also the most attractive advantage of MIT. In the past few years, epitope imprinting of proteins has achieved significant progress. Many new types of epitope-imprinted polymers with excellent properties and multifunctionalities were continuously developed by integrating the advantages of surface imprinting and advanced nanomaterials. If the amino acid sequence exposed on the surface of the protein is known, the corresponding imprinted polymers could be created by using the peptide as a template. In contrast, epitope imprinting will fail when the amino acid sequence is unknown.

2.2. Emerging special imprinting methods

2.2.1 Boronate affinity-based molecular imprinting. Compared with the above imprinting methods, boronate affinity-based molecular imprinting is a tailor-made imprinting method for glycosylated proteins by combining the boronate affinity interaction and molecular imprinting.[109] Boronic acids could display a reversible covalent reaction with *cis*-diol-containing compounds, which was the main recognition mechanism of boronate affinity interaction. When the pH of the reaction system is higher than the pK_a of boronic acid, five or six-membered cyclic esters will form. However, when the reaction medium is acidic, this boronic acid–*cis*-diol complex will dissociate.[110] Based on this reversible covalent interaction, boronic acid could be used for the specific separation of glycoproteins with a lot of *cis*-diol on the surface. Introducing boronic acids in protein imprinting could not only facilitate the immobilization and removal of templates but also provide binding sites for recognizing glycoproteins by modulating the pH. Up to now, boronate affinity-based molecular imprinting has been successfully applied for imprinting glycoproteins by combining the advantages of other imprinting methods such as surface imprinting and epitope imprinting.

Our group[111] synthesized a molecularly-imprinted monolithic column for HRP by combining boronate affinity and surface imprinting. HRP was first modified on the boronate-functionalized monolithic column and then self-polymerization of DA occurred. After the templates were removed, the resulting imprinted monolith exhibited high recognition ability toward HRP and was successfully applied in human serum, indicating a good potential in practical use. Then, our group[112] developed surface-imprinted polymers of HRP with 3-acrylamidophenylboronic acid-immobilized silica nanoparticles as the substrate. A sol–gel reaction occurred on the HRP-immobilized SiO_2@AAPBA NPs. The obtained PIPs showed good adsorption ability and high selectivity for HRP with an imprinted factor of 2.71, and further successfully separated HRP from human serum. Later, the "thiol–ene" click reaction was applied to construct PDA-coated boronate affinity-imprinted silica NPs for HRP recognition.[113] Liu *et al.*[114] applied boronic acid-modified graphene oxide (GO-APBA) as the substrate to create surface-imprinted polymers of ovalbumin (OVA). The template OVA was first modified on the GO-APBA substrate and then a sol–gel reaction occurred. To the combination of boronic acid and surface imprinting, together with a large surface area of GO, the resulting PIPs exhibited a high binding capacity of 278 mg g^{-1}, rapid adsorption kinetics of 40 min, and imprinted factor of 9.5. Sun *et al.*[115] introduced Fe_3O_4 NPs as the substrate to synthesize HRP-surface imprinted polymers with a convenient synthesis and separation procedure.

Li *et al.*[116] developed a "photolithographic boronate affinity molecular imprinting" strategy to successfully create surface-imprinted polymers toward five different glycoproteins. UV-initiated free radical polymerization occurred between the functional monomer of APBA and a crosslinker around the template glycoproteins. This method is fast, tolerant of interference, and applicable to a wide range of pH. The successful detection of a-fetoprotein (AFP) with low concentrations from human serum by MIP array-based enzyme-linked immunosorbent assay (ELISA) demonstrated the great potential for practical use in complex real samples. Then, the sample group[117] developed another facile and general "boronate affinity-based controllable oriented surface imprinting" strategy for the recognition of glycoproteins. The boronic acid pre-functionalized substrate was first used to

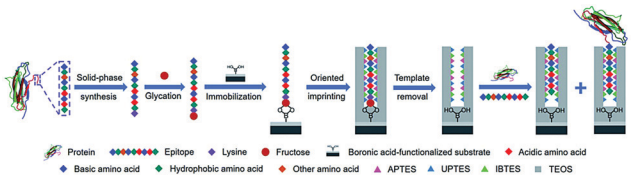

Fig. 7 Schematic of the principle and procedure of controllable oriented surface imprinting of boronate affinity-anchored epitopes. Reprinted from ref. 118.

immobilize templates and then a thickness-controllable imprinting layer was formed on the substrate by self-polymerization of DA and APBA. After the templates were removed, boronate affinity-based controllable oriented surface imprinted polymers were obtained. The affinity of such MIPs could be tuned by controlling the strength of the boronate affinity interaction by adjusting the pH. Xing *et al.*[118] introduced a new and universal strategy called "controllable oriented surface imprinting of boronate affinity-anchored epitopes" (Fig. 7). This work is the successful integration of surface imprinting, epitope imprinting, and boronate affinity. The template of glycated epitope peptide was used, which could facilitate the immobilization and removal of templates on the surface of the boronic acid-functionalized substrate. The resulting MIPs could recognize both the peptides and proteins. This method is efficient and general for creating MIPs with an affinity to proteins. Based on this work, the same group[119] proposed a new strategy called molecular imprinting and cladding (MIC) to solve the dilemma between the best affinity and best specificity for MIPs. The key to this strategy is the chemically inert cladding thin layer generated after molecular imprinting to cover the non-imprinted area. Using this strategy, a special approach termed boronate affinity-anchored epitope-oriented surface imprinting and cladding (BOSIC) was developed. The resulting cMIPs were general for the recognition of TRF, TRF receptor (TfR), AFP and carcinoembryonic antigen (CEA), and were successfully applied for fluorescence imaging of cancer cells against normal cells by targeting TfR by encapsulating fluorophore and the diagnosis of diabetes by detecting C-peptide in human urine using a dual cMIPs-based surface-enhanced Raman scattering (SERS) assay.

Overall, the boronate affinity-based molecular imprinting method is successful and tailor-made for glycosylated proteins. By integrating the advantages of other imprinting methods, a series of novel, special and general imprinting strategies based on boronate affinity interaction for glycoproteins has been developed and applied in various advanced fields such as clinical disease diagnosis and biological imaging. Although this method is only effective for glycoproteins, as a successful example of glycoprotein imprinting, its success could undoubtedly provide a lot of inspiration and thoughts for the development of protein imprinting methods, which is a general method for different proteins.

2.2.2 Solid-phase synthesis. The ultimate goal of MIT is to create highly specific MIPs, which can replace natural antibodies. To realize this goal, Piletsky group[120,121] developed a straightforward method, called "solid-phase synthesis",

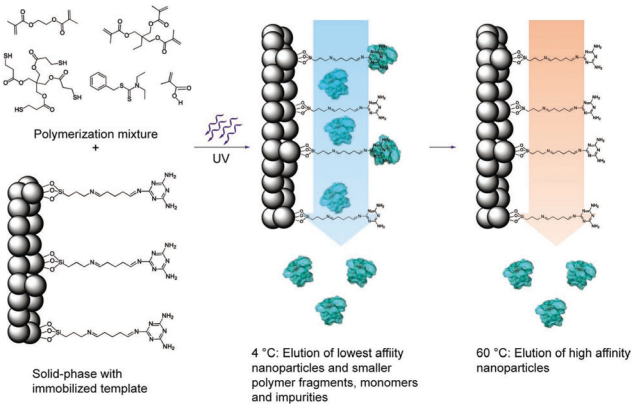

Fig. 8 Schematic representation of the solid-phase synthesis of MIP nanoparticles. The monomer mixture is injected onto the column reactor with an immobilized template and polymerization is initiated by UV-irradiation. The low-affinity particles, as well as unreacted monomers, are eluted at low temperatures. The temperature is then increased and high-affinity particles are eluted from the column for collection. Reprinted from ref. 120.

to synthesize imprinted polymer nanoparticles (nanoMIPs) with comparable size, specificity and solubility to antibodies. In a typical synthesis procedure (Fig. 8), the template-immobilized solid support (such as microsized glass beads) was incubated with monomers in organic or aqueous media. After polymerization, initiated under ultraviolet or free radical, polymer NPs were formed. To purify the MIPs NPs, the obtained polymer NPs were washed to remove lowaffinity MIPs NPs, oligomers and unreacted monomers. Finally, the nanoMIPs were obtained by eluting them from the solid support. Thermosensitive NIPAAm was often used to facilitate the release of MIPs NPs from the solid support. Compared with the traditional molecular imprinting methods, solid-phase synthesis could greatly shorten the production time and the templates were reusable. Moreover, the obtained nanoMIPs exhibited homogeneous binding sites, high specific affinity, high stability and good solubility.

By using this method, Poma *et al.*[122] constructed an automated solid-phase synthesis method for synthesizing nanoMIPs under computer control in aqueous media. Using this method, they successfully prepared nanoMIPs with specific recognition ability toward three proteins (pepsin A, trypsin and α-amylase), indicating a good potential in industrial manufacturing. However, the template proteins were modified on the solid support by covalent coupling of glutaraldehyde, which resulted in the heterogeneous recognition sites from the variation in protein orientation. Thus, Ambrosini *et al.*[123] presented a novel method to prepare nanoMIPs by using an affinity ligand (*p*-aminobenzamidine (PAB)) of protein to immobilize the template trypsin. Different from the covalent coupling, the affinity ligand endowed all the binding sites with the same orientation, thus leading to more homogeneous binding sites. The obtained nanoMIPs exhibited high specificity and selectivity toward trypsin. Based on the same strategy, Xu *et al.*[124] first formed polymer NPs on the trypsin–PAB–solid support and then modified fluorescein isothiocyanate (FITC) on the polymers NPs.

After being removed from the solid support, fluorescent MIP NPs were obtained with high affinity toward trypsin and showed almost no cross-reactivity with other proteins. Finally, the fluorescent MIP NPs were employed in a sandwich fluoroimmunoassay for the detection of trypsin with a low concentration of 50 pM spiked in human serum. The same group[125] introduced metal chelation (Cu^{2+}), inspired by PAB, to immobilize proteins with surface histidines for the fabrication of nanoMIPs by solid-phase synthesis. The IMAC interaction helped form oriented homogeneous imprinting sites on the surface of nanoMIPs. This study provides a general method for solid-phase synthesis of nanoMIPs for proteins. Then, Xu *et al.*[126] applied a cyclic 3S epitope (CGSWSNKSC) immobilized GBs as the solid support to fabricate water-soluble nanoMIPs with oriented homogeneous imprinting sites by solid-phase synthesis. The 3S cyclic epitope is the motif of the envelope glycoprotein 41 (gp41) of human immunodeficiency virus type 1 (HIV-1) and thus, the resulting anti-3S antibodies could be applied to target and block the 3S peptide of HIV-1 to prevent $CD4^+$ T cells from declining.

In the above works, microsized glass beads served as the solid support. Their low specific surface area leads to a small amount of immobilization of template proteins and the low yield of nanoMIPs. Thus, Ashley *et al.*[127] employed epoxide magnetic microspheres (FeOx@SiO_2-epoxide, 600–700 nm) as the solid support to immobilize trypsin. Because of the high specific surface area, highly abundant templates could be immobilized. Compared with conventional solid-phase synthesis, a high yield of nanoMIPs with increased 83–167 folds could be achieved by using magnetic microspheres as the solid support. Meanwhile, magnetic responsiveness facilitates the synthesis and separation procedure. This method was called ''dispersive solid-phase imprinting'' because the imprinting process was conducted on the surface of FeOx@SiO_2-epoxide, which was dispersive in the mixture. Mahajan *et al.*[128] used amino-functionalized sol–gel coated magnetic nanoparticles (magNPs) as solid support to immobilize the templates of enzymes trypsin and pepsin. A high-dilution polymerization of monomers occurred around the template on the solid support. A monomer of *N*-fluoresceinylacrylamide was added to yield fluorescent nanoMIPs with high specificity and selectivity toward the respective template proteins.

For the first time, Cecchini *et al.*[129] developed fluorescent nanoMIPs by combining solid-phase synthesis, surface imprinting, epitope imprinting and QDs. The template of the epitope peptide of human vascular endothelial growth factor (hVEGF) was immobilized on the glass beads. The resulting fluorescent nanoMIPs exhibited excellent specificity toward hVEGF, and were successfully applied in the target imaging of overexpressing hVEGF. Based on the same strategy, Gómez-Caballero *et al.*[130] synthesized nanoMIPs by using epitope peptide (C-terminus 15 amino acids sequence) of the CB1 receptor. The sizes of nanoMIPs were found to be related to temperature changes. The nanoMIPs were successfully demonstrated as artificial anti-CB1 antibodies to high selectively recognize the target proteins with 15 amino acids epitope.

Solid-phase synthesis is the most promising method to create MIPs as artificial antibodies with comparable size, specificity and solubility to antibodies. Due to its facile and automated operation, it has significant potential in industrial production. In the past few years, solid-phase synthesis has achieved some great progress, mainly emphasizing the increase of nanoMIPs yields, more homogeneous binding sites, advanced functionalities and further extending their biological applications. Many excellent solid-phase synthesis approaches have been developed to create advanced nanoMIPs by combining the advantages of other imprinting methods.

2.2.3 Post-imprinting modifications. Inspired by proteins that could acquire various functions by site-specific post-translational modifications, Takeuchi group[131–133] proposed a ''post-imprinting modification (PIM)'' method *via* site-specific chemical modifications in the imprinting cavities to endow MIPs with additional functionalities (Fig. 9). The functional monomer was modified after the templates were removed to form imprinting cavities. For example, Suga *et al.*[134] successfully transformed the binding events of PIPs toward Cyt *c* into fluorescence spectral changes. A well-designed Cyt-conjugated cleavable monomer containing a disulfide bond and a methacryl group was used as the template. Cyt *c* was removed by disulfide reduction and a fluorescent reporter molecule was then modified on the exposed thiol groups, resulting in the transduction of specific protein recognition into spectral changes. However, PIPs always suffered from heterogeneous binding sites and incomplete removal of templates. The fluorophore molecules may be inaccurately labelled on the outer side of PIPs, which will lead to high fluorescent background noise. Thus, Sunayama *et al.*[135] proposed a site-directed two-step PIM strategy to overcome this problem. A functional monomer of 4-[2-(*N*-methacrylamido)ethylaminomethyl]benzoic acid (MABA) with a secondary amine was used for PIMs. After the removal of template Lyz, the resultant PIPs were rebound with Lyz and then reacted with *p*-isothiocyanatophenyl a-D-mannopyranoside (MITC) to cap the exposed amine groups that were not located in the imprinted cavities. Based on this treatment, the bound Lyz was removed and another fluorescein isothiocyanate (FITC) was modified on the exposed amine groups in the imprinted sites. This two-step PIM strategy could greatly decrease the fluorescent background noise, thus resulting in the enhanced conversion of adsorption behaviour into fluorescence changes. Based on the above studies, the same group[136] used a multi-step PIM method to create antibody-like PIPs with a fluorescence response for the recognition of a-fetoprotein (AFP). Two different cleavable functional monomers were used for the imprinting of AFP. After the template AFP was removed, one monomer was treated as the binding site for AFP and another was modified with a fluorescent reporter molecule. The sensitive and selective detection of AFP by antibody-like PIPs could be transformed into fluorescence changes, which were beyond the natural antibodies.

Tao *et al.*[137] developed a one-step PIM strategy to fabricate a biosensor to characterize the specific recognition of glycoprotein (HRP). After the removal of the template HRP, the exposed thiol residues in the imprinted cavities were modified with boronic acid ligand by the ''thiol–ene'' click reaction. Due to the fluorescence response of the boronic acid ligand, the

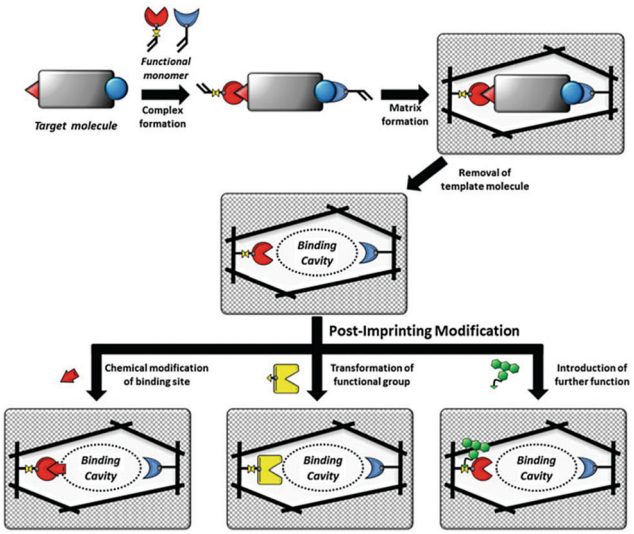

Fig. 9 Schematic illustration of MIPs and PIMs of the binding cavities of MIPs. Reprinted from ref. 132.

resulting PIPs could act as a biosensor for HRP detection by the transduction of binding events into fluorescence change. Based on their previous work,[136] Morishige *et al.*[138] created a new recognition system for AFP by PIMs. In this work, AFP was first immobilized on the surface of 4-carboxy-3-fluorophenylboronic acid (CFPBA)-functionalized support. After polymerized, AFP was removed by cleavage of disulfide bonds and cyclic diesters. Then, fluorescent dyes were functionalized with the exposed thiol groups to yield a fluorescent AFP-imprinted biosensor. The introduction of CFBA could not only facilitate the oriented immobilization of template AFP but also provide recognition sites for AFP. The successful detection of AFP in human serum demonstrated good potential in biomedical application. Wang *et al.*[139] presented a ratiometric nanosensor by PIMs for the fluorescence determination of OVA. Meanwhile, the binding result could be transformed into the visual identification on fluorescent test papers under UV (365 nm). OVA-imprinted polymers were first constructed on the SiO_2 NPs. FITC was post-modified in the imprinted cavities after the templates were removed. The resulting ratiometric nanosensor showed a detection limit of as low as 15.4 nM and could be successfully applied in real samples of human urine and chicken egg white, indicating its good potential in real applications.

The major advantage of the PIM method is to impart new functionalities to PIPs. Diverse functionalities could be introduced by various chemical derivatization based on the excellent stability of the imprinted polymers. These new functionalities will transform the recognition behaviour toward template proteins into optical or other responses, which greatly exceed more wide applications of PIPs. As discussed above, solid-phase synthesis could create nanoMIPs as artificial antibodies with comparable properties to those of natural antibodies. By using the PIM strategy, sophisticated MIP-based artificial antibodies with functionalities have the potential to go beyond natural antibodies. However, PIM also suffered from some drawbacks such as the design of complex functional monomers and tedious chemical synthesis procedures. Meanwhile, due to the unclear recognition mechanism of PIPs, the rational design of chemical modifications in the imprinted cavities should be further explored.

3. Applications of PIPs

Over the past decade, protein imprinting has achieved significant progress. Several novel imprinting methods have emerged and many protein-imprinted polymers with advanced properties have been developed, which extend their wide applications, including separation and purification, proteomics, biomarker detection, bioimaging and therapy. In this section, we focus on the recent development of PIPs in their highlighted applications.

3.1. Separation and purification

The high interferences derived from the complex components of biological samples pose great challenges for the separation of target proteins. Based on the rapid development of surface imprinting and nanomaterials, various PIPs with excellent binding capacity and selectivity were developed and applied for the separation and purification of proteins from complex biological samples such as human serum. Our group[64] synthesized Lyz–surface imprinted Silica NPs with high selectivity toward Lyz in human serum. Then, we created a thin BHb-imprinted polymer on silica NPs, which possessed a large binding capacity, high adsorption selectivity and fast binding kinetics for BHb.[65] Inspired by the excellent binding performance, the as-prepared surface-imprinted silica NPs could successfully separate BHb from cattle whole blood samples with high selectivity. Tan *et al.*[52] synthesized poly(styrenesulfonate sodium) (PSS)-assisted hierarchical bulky imprinted microparticles (denoted as PSS–PDA–MIP) of Lyz by a novel polymer-assisted hierarchically bulk imprinting strategy. Then, the as-prepared PSS–PDA–MIP possessing ultrahigh adsorption capacity of 1203.4 mg g^{-1} and high selectivity for Lyz was successfully applied for the highly selective separation of Lyz from diluted egg whites and spiked human serum. Pan *et al.*[140] fabricated multi-responsive rattle-type magnetic hollow molecular imprinted poly (ionic liquids) nanospheres with BSA as the template. The resulting Fe_3O_4@void@PILMIP were confirmed to show specific recognition ability toward BSA and were successfully applied in the separation of BSA from bovine calf serum. Yang *et al.*[141] synthesized thermo-sensitive surface-imprinted hollow nanocages with ZIF-67@Co–Fe as the substrate (Co–Fe@CBMA–MIPs) for the recognition of BSA. ZIF-67@Co–Fe provided a high specific surface area and Co–Fe double ions facilitated the immobilization and removal of the templates. Under optimum adsorption conditions, the Co–Fe@CBMA–MIPs displayed a high binding capacity of 520.35 mg g^{-1}, rapid binding kinetics of 50 min, and imprinting factor of 8.55. Encouraged by their excellent binding performance, these PIPs could successfully separate BSA from fetal bovine serum. Bhakta *et al.*[72] applied antibody-like

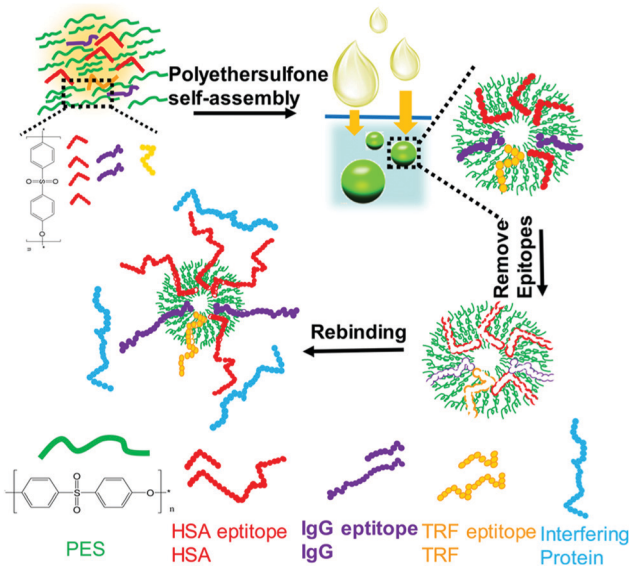

Fig. 10 Fabrication of multiepitope templates imprinted particles *via* PES self-assembly and application in the simultaneous capture of various target proteins. Reprinted from ref. 103.

magnetic surface imprinted polymers to separate HSA. Benefiting from the magnetic responsiveness and high binding capacity, the resulting PIPs achieved the removal of ~88% of albumin from human serum. Yang *et al.*[102] successfully applied transferrin (TRF) epitope-imprinted PES beads for a human plasma proteome analysis and quantification for the first time. Then, the same group[103] fabricated multiepitope imprinted PES particles to simultaneously capture three proteins (HSA, TRF, and IgG) from the complex human plasma, indicating the promising potential in practical applications (Fig. 10). Li *et al.*[106] further proposed an EI-IMAC strategy to design surface epitope imprinting polymers with His-tag epitope as a template. The resulting PIPs possessed fast adsorption kinetics (15 min) and a high imprinting factor (7.1). Compared with the IMAC strategy, this strategy exhibited increased purity (~5%) for His-tagged recombinant proteins separated from crude cell lysis. Weerasuriya *et al.*[142] presented a new strategy to create surface-imprinted silica-coated magnetic NPs with protein (PrA)-like nanopockets for the purification of IgG antibodies. Mouse IgG_{2a}, which is the binding partner of PrA, was used as the template. A sol–gel reaction of organosilane monomers occurred around the templates. After capping the nonbinding sites and removing the templates, the resulting PIPs showed PrA-like specific recognition of IgG. Rough core–shell NPs were found to possess a high binding capacity and better selectivity than the commercial PrA magnetic beads. These PIPs are cost-effective, reusable, stable, and the first report to mimic PrA recognition to purify antibodies.

3.2. Proteomics

To date, mass spectrometry (MS) has become a powerful and popular tool for proteomic analysis because of its high resolution, high throughput, high sensitivity, and high accuracy. However, the analysis of complex biological samples by MS still remains a great challenge. This is because the complex components of biological samples often lead to signal interference, and greatly suppress the MS ionization of target proteins. Thus, prior to MS analysis, highly selective separation of target proteins from complex biological samples is urgently needed. Protein imprinted polymers featured by excellent selectivity have great potential for MS analysis of complex biological samples.

Wan *et al.*[143] for the first time-developed PIPs to highly separate target proteins for matrix-assisted laser desorption/ionization time-of-flight mass spectrometry (MALDI-TOF MS) analysis. The self-polymerization of DA occurred around the template Lyz. After the templates were removed, thin Lyz-imprinted polymers were introduced on the Fe_3O_4@SiO_2 NPs to yield Lyz-surface imprinted magnetic NPs (Lyz-MIPs). Lyz-MIPs showed excellent binding capacity and high selectivity for Lyz, then applied to highly selectively separate Lyz from diluted egg white samples for MALDI-TOF MS analysis. The enhanced effect of MALDI-TOF MS signals for Lyz was demonstrated after the selective separation procedure *via* Lyz-MIPs. Bertolla *et al.*[144] proposed a fast and easy online method for target protein analysis by integrating PIPs with MALDI-TOF MS. Poly-(acrylamido)-derivative (PAD) nanoMIPs were synthesized using human serum transferrin (HTR) as the template. The resulting solvent-responsive PAD-nanoMIPs not only showed specific recognition ability toward HTR but also could release *in situ* the bound HTR from the PAD-nanoMIPs-target-plate by adding acetonitrile for MALDI-TOF MS analysis. This PAD-nanoMIPs/MALDI-TOF MS analysis platform could successfully detect HTR from a real sample of serum, indicating its great potential in clinical diagnosis and targeted proteomics. Cyt *c*, which is important in cell apoptosis and can interact with anti-apoptosis proteins, which leads to the effect of functions. Two pivotal anti-apoptosis proteins of HSP27 and Bcl-xL could interact with Cyt *c*. Based on these findings, to study Cyt *c*-HSP27 and Cyt *c*-Bcl-xL interactions, Zhang *et al.*[145] developed a simultaneous quantification method by combining protein imprinting and an LC-MS/MS method (Fig. 11). The template of the epitope peptide of Cyt *c* was used to synthesize Cyt *c*-surface imprinted silica NPs. The binding performance, including adsorption capacity, binding kinetics and selectivity was confirmed in detail. Compared with the Co-IP/Western Blotting, this combinational approach could successfully quantitatively analyse the protein–protein interactions within Cyt *c* and two anti-apoptosis proteins in a different complex biological sample of breast cancer cells.

3.3. Biomarker detection

PIPs, which are considered synthetic antibodies, have also been used as recognition materials for protein biomarker detection from complex pathological samples. Based on their previous work,[117] Bi *et al.*[146] developed boronate affinity imprinted microplates as ELISA to detect AFP. 4-Formylphenylboronic acid (FPBA) was first functionalized on the bottom of the well and walls of a 96-well microplate. Then, the template glycoproteins were immobilized on the basis of the boronate affinity

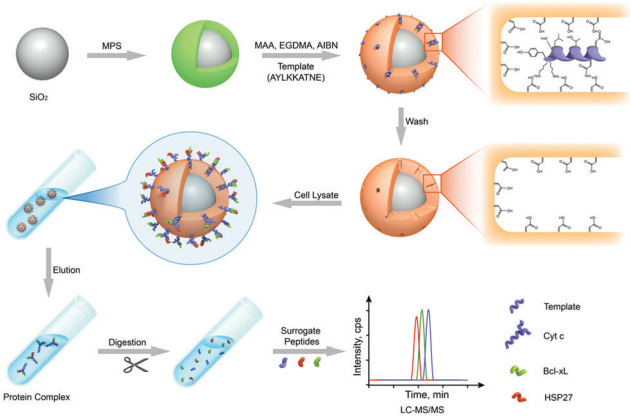

Fig. 11 Schematic representation of MIPs coupled with LC-MS/MS-based targeted proteomics for the simultaneous quantification of Cyt *c* interactions with HSP27 and Bcl-xL. Reprinted from ref. 145.

interactions, and self-copolymerization of aniline in water occurred around the templates. After the removal of the templates in acid media, glycoprotein-imprinted microplates were obtained with the appropriate thickness of imprinted layers. This strategy was first demonstrated by the excellent binding performance of PIPs with standard HRP as an imprinting template. Finally, a PIPs-based sandwich ELISA was constructed for the detection of AFP by integrating with AFP-imprinted microplates. Under the optimal analysis condition, a concentration of 12 ± 2.0 ng mL^{-1} for AFP in human serum was detected by this ELISA, which corresponded to the result (10 ng mL^{-1}) obtained by radioimmunoassay. However, because of the use of specific antibodies and biological reagents, this ELISA was not stable and expensive. Thus, based on their previous work,[116] the same group[147] further developed a novel boronate-affinity sandwich assay (BASA) for AFP analysis by integrating photolithographic boronate-affinity molecular imprinting with boronate-affinity based SERS probe (AgNPs) (Fig. 12). Standard HRP was first selected as the template to evaluate the binding performance of BASA. The practical potential of this BASA was then demonstrated by the AFP-imprinted BASA. To the human serum containing AFP with a known concentration of 12.0 ± 2.0 ng mL^{-1}, the concentration of 13.8 ± 3.3 ng mL^{-1} was determined by the AFP-imprinted BASA. This approach is stable, fast, cost-effective, and has great potential in clinical diagnostics with high throughput. Patra *et al.*[148] developed a trace prostate-specific antigen (PSA)

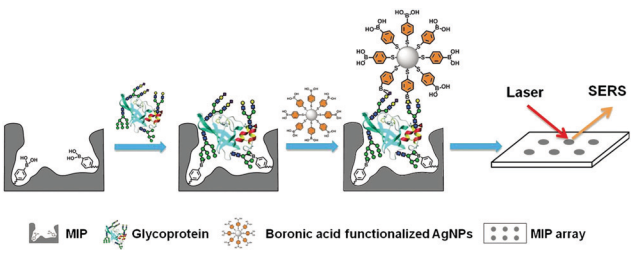

Fig. 12 Schematic representation of the boronate-affinity sandwich assay of glycoproteins. Reprinted from ref. 147.

electrochemical sensor by combining protein–surface imprinted polymers and nanomaterials. MnO_2-Nanoparticles were modified on the surface of MWCNTs to yield MnO_2-nanoparticle decorated MWCNTs-iniferter. This iniferter was attached to a pencil graphite electrode (PGE) and then a controlled radical polymerization occurred with the existence of the template PSA. After the templates were removed, a PSA-imprinted electrochemical sensor was obtained. The detecting limit of this PSA-sensor by the square wave stripping voltammetric (SWSV) technique was 0.25 pg L^{-1}, and 3.04 pg L^{-1} by the differential pulse stripping voltammetric (DPSV) technique. The successful detection of PSA in men and women samples of serum, urine, and forensic by the as-prepared sensor was demonstrated using the commercially available ELISA, indicating the great potential in the clinical diagnosis of PSA. Shumyantseva *et al.*[149] synthesized myoglobin (Mb)-imprinted polymers on the MWCNTs-modified electrodes for the sensitive detection of Mb in undiluted human plasma samples. Based on this Mb-electrochemical sensor, plasma samples could be accurately classified and referred to related groups of healthy donors (HDs) and patients with acute myocardial infarction (AMI) by combining the multi-parameter electrochemical analysis and computational cluster assay. Compared with other standard immunochemical methods for Mb detection, this approach is facile, fast, cost-effective, and showed excellent potential in personalized medicine such as "point-of-care" biosensors. Karami[150] constructed a novel and low-cost dual-modality immunosensor for the simultaneous detection of PSA and Mb by combining protein–surface imprinting and nanocomposite (NCP)-based biosensing layer. Protein–surface imprinted polymers were fabricated with a gold screen-printed electrode (SPE) as the substrate, on which radical polymerization occurred with ethylene glycol dimethacrylate as a crosslinker, methyl acrylate as the monomer, PSA and Mb as dual-templates. After the templates were removed, PIP-SPE was formed with specific sensing for both PSA and Mb. Fe_3O_4 NPs were successively modified with MWCNTs, GO and specific antibodies for PSA (Ab) to yield the NCP-based biosensing material. To simultaneously detect PSA and Mb, PIP-SPE was first used to recognize PSA and Mb, and their binding signal was sent as an output to electrochemical impedance spectroscopy (EIS). This was followed by adding the NCP-based sensing material to PIP-SPE, another EIS signal was obtained from the immune reaction between PSA-bound SPE and NCP. The EIS signal of Mb was calculated by the differences in the EIS signal of the two steps. This dual-modality immunosensor exhibited high specificity and selectivity toward PSA and Mb and possessed a low detecting limit of 5.4 pg mL^{-1} for PSA and 0.83 ng mL^{-1} for Mb. Finally, this novel immunosensor was successfully applied to simultaneously analyse PSA and Mb in human serum and urine samples, indicating a great potential in disease diagnosis of multi-biomarkers.

3.4. Bioimaging and therapy

PIPs are alternatives to natural antibodies for biological recognition, but also possess a lot of advantages including high stability, low cost, and ease of functionalization, which can introduce fluorescence or better biocompatibility. Thus, PIPs

hold good potential in target bioimaging and therapy, in which PIPs could specifically recognize corresponding biomarkers in cancer cells and release the loaded drugs.

Liu *et al.*[151] made the first attempt to employ PIPs as antibody-like NPs to specifically sequestrate target proteins in living cells. With an initiator of 4,4′-azobis-(4-cyanopentanoic acid) (ACPA) functionalized Fe_3O_4@SiO_2 NPs as the substrate, a facile polymerization occurred around the template protein (DNase I) to yield protein–surface imprinted polymers with high hydrophilicity and biocompatibility. The use of NIPAm endowed the PIPs with thermo-responsiveness toward temperature changes, and the fluorescent monomer provided fluoresce quenching when PIPs rebound with target proteins. The resulting Fe_3O_4@SiO_2@MIP ANPs presented excellent aqueous dispersion stability with an average size (85 nm). The introduction of magnetic cores not only facilitated the synthesis and separation but also offered the magnetic manipulation of PIPs within cells. After confirming the good adsorption specificity and selectivity, the as-prepared Fe_3O_4@SiO_2@MIP ANPs were successfully applied to the specific sequestration of target proteins in living cells without disruption. This study has good potential in the study of protein functions in cells and medical diagnosis. Cecchini *et al.*[129] developed fluorescent nanoMIPs for the specific recognition of hVEGF and further targeting imaging of its overexpression (Fig. 13). The integration of QDs in the PIP-hybrid nanoprobes provided fluorescence quenching against the recognition of nanoMIPs toward hVEGF. The resulting QD-PIPs hybrid nanoprobes exhibited specific recognition and good binding selectivity toward hVEGF *in vitro* and were finally applied to target imaging of overexpressing hVEGF in zebrafish embryos for the xenotransplantation of human melanoma cells. Zhang *et al.*[152] prepared core–shell protein–surface imprinted polymers to specifically recognize epidermal growth factor receptor (EGFR) by integrating surface imprinting with epitope imprinting. The template of the epitope peptide of EGFR was bonded with palmitic acid, then a reverse microemulsion polymerization occurred on the surface of CD-embedded silica NPs with acrylamide as the functional monomer and *N*,*N*-methylenebisacrylamide as the crosslinker. The resulting CD-embedded PIPs exhibited fluorescence quenching against the rebinding with EGFR and showed high adsorption selectivity and sensitivity for EGFR. In the *in vitro* experiments, HeLa cells with high expression of EGFR could be accurately targeted and distinguished by the CDs-embedded PIPs, which showed stronger fluorescence than that in MCF-7 cells with low high expression of EGFR. Inspired by the good performance *in vitro* experiment, the CD-embedded PIPs were further successfully used for the target imaging of tumour cells with overexpressing EGFR in mice. Guo *et al.*[153] developed a general approach called reverse microemulsion-confined epitope-oriented surface imprinting and cladding (ROSIC) to fabricate coreless and core/shell NPs with specific target capability toward proteins and peptides. A series of NPs, including QDs, SPMNPs (superparamagnetic NPs), AgNPs and UCNPs were used as substrates to obtain a variety of size controllable dual-functional single-core@cMIP NPs. Finally, QD@cMIP NPs were applied to demonstrate the potential in cancer cell target imaging. With specificity toward two typical cancer biomarkers, including human epidermal growth factor receptor-2 (HER2) and transmembrane glycoprotein non-metastatic gene B (GPNMB), QD@cMIP NPs could successfully differentiate triple-negative breast cancer (TNBC) cells from other cell lines *via* fluorescence imaging. The practical potential was demonstrated by *in vivo* target imaging of TNBC-bearing mice.

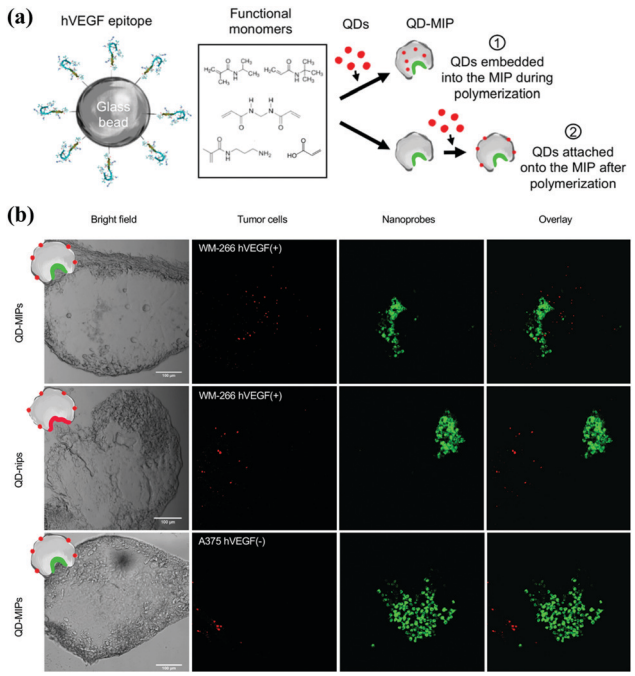

Fig. 13 (a) Schematic of the two strategies exploited to produce QD-MIPs, based on solid-phase synthesis: (i) embedding the QDs in the MIP matrix during its polymerization; (ii) attaching the QDs onto the nanoMIPs after the polymerization process. (b) A panel of bright field and fluorescence images of human melanoma cells (WM-266 hVEGF(+) model and A-375 hVEGF(−) model) (green) and the fluorescent nanoprobes (red), acquired with a confocal microscope Leica SP2 (scale bar 100 μm), and the overlay of the two signal. Reprinted from ref. 129.

In addition to target cell imaging, PIPs also could load drugs and control their release for cancer therapies.[154–163] Canfarotta *et al.*[154] developed dual-template imprinted polymers to achieve the specific recognition of cancer cells and further result in specific drug release. Solid-phase synthesis was applied to prepare doxorubicin (DOX)-loaded nanoMIPs with an epitope peptide of EGFR and doxorubicin as the dual-templates. The specific recognition ability and adsorption selectivity of the nanoMIPs was first confirmed. Based on the specific recognition of EGFR on cancer cells, the DOX-loaded nanoMIPs could specifically release DOX in cancer cells with overexpressing EGFR to elicit their cytotoxicity and apoptosis. Qin *et al.*[155] then synthesized imprinted polymers of dual-templates for the target recognition toward cell membrane proteins to achieve simultaneous target imaging and therapy by specific drug release for cells. The DOX-loaded fluorescent PIPs (FMIPs@DOX) were synthesized by using fluorescent Si@SiO_2@MPS NPs as the substrate, epitope peptide of membrane protein (P32)

and DOX as the double templates. In an *in vitro* experiment, the FMIPs@DOX was successfully applied for the target imaging of 4T1 cancer cells based on the specific recognition between FMIPs@DOX and high expression P32 proteins. Moreover, only the 4T1 cancer cells with overexpressing P32 proteins were elicited to apoptosis after the release of DOX. Then, FMIPs@DOX was further intravenously injected into tumour-bearing mice for therapy, which was demonstrated to exhibit almost the same anti-tumour effects compared with the intratumoral injection. Peng *et al.*[156] prepared double-template imprinted polymers with multifunctionalities, including specific recognition of cancer cells, target fluorescence imaging, magnetic resonance (MR) imaging, specific drug release, chemotherapy and photodynamic (PD) therapy (Fig. 14). The DOX-loaded PIPs (MIPs@DOX) were formed with $FSiO_2$@MPS encapsulating gadolinium-doped silicon quantum dots (Si_{Gd}QDs) and chlorin e6 (Ce6) as the substrate and using the epitope peptide of CD59 protein and DOX as the dual templates. The introduction of Si_{Gd}QDs led to fluorescence and MR imaging, and the Ce6 could produce reactive oxygen species (ROS) for PD therapy. The MIPs@DOX were confirmed to specifically recognize cancer cells with high expression of CD59 for target imaging, and the DOX released from the MIPs@DOX and high abundance of ROS generated by light irradiation were integrated as a synergistic therapy effect for cancer cells. The target imaging and synergistic therapy were both demonstrated by *in vitro* and *in vivo* tests. The same group[157] then developed novel DOX-loaded PIPs (FZIF-8/DOX-MIPs) with biodegradable effects in the tumour microenvironment. The FZIF-8/DOX-MIPs were fabricated on the surface of ZIF-8, which encapsulated CDs and DOX, and applied epitope peptide of protein (CD59) as the template.

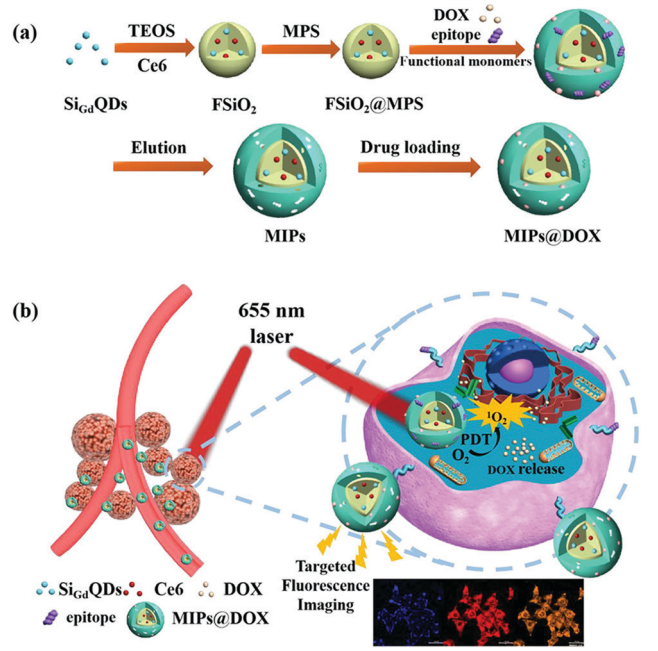

Fig. 14 (a) Schematic illustration for the preparation of MIPs@DOX; (b) Schematic illustration of MIPs@DOX for targeted chemo-photodynamic synergistic treatment of tumour *in vivo*. Reprinted from ref. 156.

The disulfide bond in the crosslinker of *N*,*N*′-diacrylylcystamine (BAC) will be broken at a high concentration of glutathione, and the monomer of dimethylaminoethyl methacrylate (DMAEMA) will swell at low pH. Together with the instability of ZIF-8 in weak acid, GSH/pH dual-stimulation was formed to achieve controllable drug release. Finally, the FZIF-8/DOX-MIPs exhibited target fluorescence imaging, and further specific and controllable drug release toward cancer cells with overexpressing CD59, which were validated by *in vitro* and *in vivo* tests. Lu *et al.*[163] synthesized sialic acid (SA)-imprinted biodegradable NPs (BS-NPs) by the boronate-affinity-controllable oriented surface imprinting approach. Cytotoxic ribonuclease A (RNase A) was pre-caged in the matrix of disulfide-hybridized silica NPs as nanovectors, which could be degraded under the GSH triggering. The prepared SA-imprinted RNase A@BS-NPs thus could selectively target SA-overexpressed tumor cells and was subsequently biodegraded by GSH to release RNase A to enhance cell cytotoxicity. The *in vitro* and *in vivo* experiments demonstrated the practical potential of SA-imprinted RNase A@BS-NPs in specific targeting and therapeutic efficiency toward cancer cells.

4. Conclusion and future perspectives

In summary, a comprehensive review of the recent advances in protein imprinting methods and their highlighted applications is presented. Various novel protein imprinting methods have been developed to solve the remaining bottlenecks that traditional imprinting methods could not address. Nanomaterial-based surface imprinting of proteins could improve the binding performance of PIPs, including adsorption capacity, binding kinetics, sensitivity and selectivity. The use of epitope templates instead of the whole proteins in epitope imprinting could almost address all the problems derived from the inherent properties of proteins, which greatly increased the success and applicability of molecular imprinting for proteins. Solid-phase synthesis provides a great potential in the scalable synthesis of nanoMIPs with properties comparable to natural antibodies. Meanwhile, advanced multifunctionalities could be imparted into PIPs through the introduction of functional nanomaterials and post-imprinting modification, which make PIPs possible to go beyond natural antibodies. Combining the advantages of these protein imprinting methods, special boronate affinity-based molecular imprinting has been successful for glycoproteins. Based on the excellent properties and advanced multifunctionalities, the traditional application of PIPs in separation and purification has evolved into several advanced fields, including proteomics, biomarker detection, target bioimaging and therapy.

Despite making significant progress, there are still several challenges that are remaining to be resolved in protein imprinting. First, the recognition mechanism between the templates and functional monomers is still obscure and rarely explored. More attention and designed experiments are needed to study the recognition process, which will be beneficial to the synthesis of PIPs and greatly stimulate their development. Second, some problems in the synthesis process also limit the development of

protein imprinting. For example, synthesis conditions must be optimised to maintain the conformation and solubility of proteins. As for the use of epitope peptides as a template, the acquisition of epitope peptides of proteins with an unknown amino acid sequence is an unavoidable issue. The immobilization of templates with different orientations will also cause non-specific adsorption derived from the heterogeneous binding sites. Third, the reported PIPs were mostly limited to a standard protein, a general protein imprinting method, which is applicable to different proteins should be explored. Finally, exploring the potential of PIPs as synthetic receptor/antibody in biomedical applications is still in an early stage.

According to the above discussion, it can be anticipated that the development of protein imprinting in the near future will be carried out in two aspects: on the one hand, more PIPs with excellent binding performances will be designed for the separation and recognition of proteins by the introduction of advanced nanomaterials and novel protein imprinting methods. On the other hand, various multifunctional nanoMIPs will be continuously created for biomedical applications by combining the advantages of several imprinting methods such as solid-phase imprinting, epitope imprinting, and surface imprinting, and thus demonstrating the potential of PIPs as synthetic antibodies to replace or even go beyond natural antibodies. As an interdisciplinary field, the rapid development of material science, omics, and life science will provide great opportunities for the development of protein imprinting and will further extend their advanced application fields.

Author contributions

Yanting He: conceptualization and writing the original draft preparation; Zian Lin: funding acquisition, conceptualization, editing and supervision.

Conflicts of interest

There are no conflicts to declare.

Acknowledgements

This work was supported by the National Natural Science Foundation of China (21974021 and 22036001), and the Major Project of Science and Technology of Fujian Province (2020HZ06006).

Notes and references

1 N. M. Bergmann and N. A. Peppas, *Prog. Polym. Sci.*, 2008, **33**, 271–288.
2 Y. J. Cao, M. Zheng, W. H. Cai and Z. C. Wang, *Chin. Chem. Lett.*, 2020, **31**, 463–467.
3 H. K. Li, H. L. Ye, X. X. Zhao, X. L. Sun, Q. Q. Zhu, Z. Y. Han, R. R. Yuan and H. M. He, *Chin. Chem. Lett.*, 2021, **32**, 2851–2855.
4 J. R. Clegg and N. A. Peppas, *Soft Matter*, 2020, **16**, 856–869.
5 A. A. Shukla and J. Thoemmes, *Trends Biotechnol.*, 2010, **28**, 253–261.
6 A. L. Bole and P. Manesiotis, *Adv. Mater.*, 2016, **28**, 5349–5366.
7 M. Cieplak and W. Kutner, *Trends Biotechnol.*, 2016, **34**, 922–941.
8 H. Asanuma, T. Hishiya and M. Komiyama, *Adv. Mater.*, 2000, **12**, 1019–1030.
9 B. Sellergren, *TrAC, Trends Anal. Chem.*, 1997, **16**, 310–320.
10 F. Breinl and F. Haurowitz, *Physiol. Chem.*, 1930, **192**, 45–57.
11 S. Mudd, *J. Immunol.*, 1932, **23**, 423–427.
12 M. V. Polyakov, *Zhur. Fiz. Khim.*, 1931, **2**, 799–805.
13 L. Pauling, *J. Am. Chem. Soc.*, 2002, **62**, 2643–2657.
14 F. H. Dickey, *Proc. Natl. Acad. Sci. U. S. A.*, 1949, **35**, 227–229.
15 G. Wulff and A. Sarhan, *Angew. Chem., Int. Ed. Engl.*, 1972, **11**, 341–346.
16 K. Mosbach, *Trends Biochem. Sci.*, 1994, **19**, 9–14.
17 C. Alexander, H. S. Andersson, L. I. Andersson, R. J. Ansell, N. Kirsch, I. A. Nicholls, J. O'Mahony and M. J. Whitcombe, *J. Mol. Recognit.*, 2006, **19**, 106–180.
18 G. Vasapollo, R. Del Sole, L. Mergola, M. R. Lazzoi, A. Scardino, S. Scorrano and G. Mele, *Int. J. Mol. Sci.*, 2011, **12**, 5908–5945.
19 L. X. Chen, S. F. Xu and J. H. Li, *Chem. Soc. Rev.*, 2011, **40**, 2922–2942.
20 R. Kecili and C. M. Hussain, *Int. J. Anal. Chem.*, 2018, **2018**, 8503853.
21 E. Turiel and A. Martin-Esteban, *Anal. Chim. Acta*, 2010, **668**, 87–99.
22 J. P. Schillemans and C. F. van Nostrum, *Nanomedicine*, 2006, **1**, 437–447.
23 S. N. He, L. P. Zhang, S. K. Bai, H. Yang, Z. Cui, X. F. Zhang and Y. P. Li, *Eur. Polym. J.*, 2021, **143**, 110179.
24 N. Leibl, K. Haupt, C. Gonzato and L. Duma, *Chemosensors*, 2021, **9**, 123.
25 J. Wackerlig and P. A. Lieberzeit, *Sens. Actuators, B*, 2015, **46**, 144–157.
26 B. Amma, B. Sjb, B. Spw and B. Jb, *TrAC, Trends Anal. Chem.*, 2021, **144**, 116431.
27 R. R. Xing, Y. R. Wen, H. He, Z. C. Guo and Z. Liu, *TrAC, Trends Anal. Chem.*, 2019, **110**, 417–428.
28 J. J. Xu, H. H. Miao, J. X. Wang and G. Q. Pan, *Small*, 2020, **16**, 1906644.
29 K. Haupt, P. Ra Ngel and B. Bui, *Chem. Rev.*, 2020, **120**, 9554–9582.
30 H. Q. Zhang, *Adv. Mater.*, 2020, **32**, 1806328.
31 Z. El-Schich, Y. Zhang, M. Feith, S. Beyer and A. G. Wingren, *Biotechniques*, 2020, **69**, 406–419.
32 N. Zhang, Y. R. Xu, Z. L. Li, C. R. Yan, K. Mei, M. L. Ding, S. C. Ding, P. Guan, L. W. Qian, C. B. Du and X. L. Hu, *Macromol. Rapid Commun.*, 2019, **40**, 1900096.
33 A. N. Peppas and R. D. Kryscio, *Acta Biomater.*, 2012, **8**, 461–473.

34 X. H. Ma, J. P. Li, C. Wang and G. B. Xu, *Chin. J. Anal. Chem.*, 2016, **44**, 152–159.
35 S. Li, S. Cao, M. J. Whitcombe and S. A. Piletsky, *Prog. Polym. Sci.*, 2014, **39**, 145–163.
36 H. R. Culver and N. A. Peppas, *Chem. Mater.*, 2017, **29**, 5753–5761.
37 M. Dinc, C. Esen and B. Mizaikoff, *TrAC, Trends Anal. Chem.*, 2019, **114**, 202–217.
38 X. D. Wang, G. Chen, P. Zhang and Q. Jia, *Anal. Methods*, 2021, **13**, 1660–1671.
39 T. Khumsap, A. Corpuz and L. T. Nguyen, *RSC Adv.*, 2021, **11**, 11403–11414.
40 C. Boitard, A. Bée, C. Menager and N. Griffete, *J. Mater. Chem. B*, 2018, **6**, 1563–1580.
41 M. Glad, O. Norrlöw, B. Sellergren, N. Siegbahn and K. Mosbach, *J. Chromatogr. A*, 1985, **347**, 11–23.
42 O. Brüggemann, K. Haupt, Y. Lei, E. Yilmaz and K. Mosbach, *J. Chromatogr. A*, 2000, **889**, 15–24.
43 P. A. Lieberzeit, S. Gazda-Miarecka, K. Halikias, C. Schirk, J. Kauling and F. L. Dickert, *Sens. Actuators, B*, 2005, **111**, 259–263.
44 E. Gizem and M. Bo, *Sensors*, 2017, **17**, 288.
45 A. Mujahid, N. Iqbal and A. Afzal, *Biotechnol. Adv.*, 2013, **31**, 1435–1447.
46 A. L. Hillberg and M. Tabrizian, *IRBM*, 2008, **29**, 89–104.
47 M. J. Whitcombe, I. Chianella, L. Larcombe, S. A. Piletsky, J. Noble, R. Porter and A. Horgan, *Chem. Soc. Rev.*, 2011, **40**, 1547–1571.
48 K. G. Yang, S. W. Li, L. K. Liu, Y. W. Chen and W. Zhou, *Adv. Mater.*, 2019, **31**, 1902048.
49 N. Zhang, X. L. Hu, P. Guan, C. B. Du, J. Li, L. W. Qian, X. Y. Zhang, S. C. Ding and B. P. Li, *Chem. Eng. J.*, 2017, **317**, 356–367.
50 C. Boitard, A. L. Rollet, C. Ménager and N. Griffete, *Chem. Commun.*, 2017, **53**, 8846–8849.
51 Y. N. Yuan, C. L. Yang, T. W. Lv, F. X. Qiao, Y. Zhou and H. Y. Yan, *Anal. Chim. Acta*, 2018, **1033**, 213–220.
52 S. Y. Tan, Y. Long, Q. Han, J. D. Wang, Q. L. Liang and M. Y. Ding, *ACS Appl. Bio Mater.*, 2018, **2**, 388–396.
53 H. Shi, W. B. Tsai, M. D. Garrison, S. Ferrari and B. D. Ratner, *Nature*, 1999, **398**, 593–597.
54 J. Kalecki, Z. Iskierko, M. Cieplak and P. S. Sharma, *ACS Sens.*, 2020, **5**, 3710–3720.
55 P. Zahedi, M. Ziaee, M. Abdouss, A. Farazin and B. Mizaikoff, *Poly. Adv. Technol.*, 2016, **27**, 1124–1142.
56 M. Pan, L. Hong, X. Xie, K. Liu, J. Yang and S. Wang, *Macromol. Chem. Phys.*, 2021, **222**, 2000222.
57 B. D. Gupta, A. M. Shrivastav and S. P. Usha, *Sensors*, 2016, **16**, 1381.
58 X. Guo, J. Li, M. Arabi, X. Wang, Y. Wang and L. Chen, *ACS Sens.*, 2020, **5**, 601–619.
59 H. R. Culver, S. D. Steichen and N. A. Peppas, *Biomacromolecules*, 2016, **17**, 4045–4053.
60 Y. Lv, T. Tan and F. Svec, *Biotechnol. Adv.*, 2013, **31**, 1172–1186.
61 X. Ding and P. A. Heiden, *Macromol. Mater. Eng.*, 2014, **299**, 268–282.
62 M. Niu, C. Pham-Huy and H. He, *Microchim. Acta*, 2016, **183**, 2677–2695.
63 G. Fu, H. He, Z. Chai, H. Chen, J. Kong, Y. Wang and Y. Jiang, *Anal. Chem.*, 2011, **83**, 1431–1436.
64 Z. Lin, Z. Xia, J. Zheng, D. Zheng, L. Zhang, H. Yang and G. Chen, *J. Mater. Chem.*, 2012, **22**, 17914–17922.
65 Z. Xia, Z. Lin, Y. Xiao, L. Wang, J. Zheng, H. Yang and G. Chen, *Biosens. Bioelectron.*, 2013, **47**, 120–126.
66 J. Liu, K. Yang, Q. Deng, Q. Li, L. Zhang, Z. Liang and Y. Zhang, *Chem. Commun.*, 2011, **47**, 3969–3971.
67 A. Nematollahzadeh, W. Sun, C. S. Aureliano, D. Lütkemeyer, J. Stute, M. J. Abdekhodaie, A. Shojaei and B. Sellergren, *Angew. Chem., Int. Ed.*, 2011, **50**, 495–498.
68 S. Bhakta, M. S. I. Seraji, S. L. Suib and J. F. Rusling, *ACS Appl. Mater. Interfaces*, 2015, **7**, 28197–28206.
69 Z. Zhang, X. Zhang, D. Niu, Y. Li and J. Shi, *J. Mater. Chem. B*, 2017, **5**, 4214–4220.
70 W. H. Zhou, C. H. Lu, X. C. Guo, F. R. Chen, H. H. Yang and X. R. Wang, *J. Mater. Chem.*, 2010, **20**, 880–883.
71 R. Gao, X. Kong, X. Wang, X. He, L. Chen and Y. Zhang, *J. Mater. Chem.*, 2011, **21**, 17863–17871.
72 S. Bhakta, C. K. Dixit, I. Bist, J. Macharia, M. Shen, K. Kadimisetty, J. He, B. Dutta, S. L. Suib and J. F. Rusling, *Chem. Commun.*, 2017, **53**, 9254–9257.
73 J. Zhou, Y. Wang, J. Bu, B. Zhang and Q. Zhang, *ACS Appl. Mater. Interfaces*, 2019, **11**, 25682–25690.
74 Y. Li, H. H. Yang, Q. H. You, Z. X. Zhuang and X. R. Wang, *Anal. Chem.*, 2006, **78**, 317–320.
75 R. Ouyang, J. Lei and H. Ju, *Chem. Commun.*, 2008, 5761–5763.
76 T. Chen, M. Shao, H. Xu, S. Zhuo, S. Liu and S. T. Lee, *J. Mater. Chem.*, 2012, **22**, 3990–3996.
77 M. Zhang, J. Huang, P. Yu and X. Chen, *Talanta*, 2010, **81**, 162–166.
78 C. Zheng, X. L. Zhang, W. Liu, B. Liu, H. H. Yang, Z. A. Lin and G. N. Chen, *Adv. Mater.*, 2013, **25**, 5922–5927.
79 M. Liu, J. Pi, X. Wang, R. Huang, Y. Du, X. Yu, W. Tan, F. Liu and K. J. Shea, *Anal. Chim. Acta*, 2016, **932**, 29–40.
80 Y. P. Qin, D. Y. Li, X. W. He, W. Y. Li and Y. K. Zhang, *ACS Appl. Mater. Interfaces*, 2016, **8**, 10155–10163.
81 X. Xu, P. Guo, Z. Luo, Y. Ge, Y. Zhou, R. Chang, W. Du, C. Chang and Q. Fu, *RSC Adv.*, 2017, **7**, 18765–18774.
82 Z. Yang, J. Xu, J. Wang, Q. Zhang and B. Zhang, *Chem. Eng. J.*, 2019, **373**, 923–934.
83 Z. Yang, J. Chen, J. Wang, Q. Zhang and B. Zhang, *ACS Sustainble. Chem. Eng.*, 2020, **8**, 3241–3252.
84 J. Luo, S. Jiang and X. Liu, *J. Phys. Chem. C*, 2013, **117**, 18448–18456.
85 F. Chen, W. Zhao, J. Zhang and J. Kong, *Phys. Chem. Chem. Phys.*, 2016, **18**, 718–725.
86 J. Guo, Y. Wang, Y. Liu, C. Zhang and Y. Zhou, *Talanta*, 2015, **144**, 411–419.
87 J. Luo, J. Huang, J. Cong, W. Wei and X. Liu, *ACS Appl. Mater. Interfaces*, 2017, **9**, 7735–7744.
88 M. Sobiech, P. Bujak, P. Luliński and A. Pron, *Nanoscale*, 2019, **11**, 12030–12074.

89 M. Díaz-Álvarez and A. Martín-Esteban, *Biosensors*, 2021, **11**, 79.
90 P. P. Tang and J. B. Cai, *Chin. J. Chem. Phys.*, 2010, **23**, 195.
91 W. Zhang, X. W. He, Y. Chen, W. Y. Li and Y. K. Zhang, *Biosens. Bioelectron.*, 2011, **26**, 2553–2558.
92 W. Zhang, X. W. He, Y. Chen, W. Y. Li and Y. K. Zhang, *Biosens. Bioelectron.*, 2012, **31**, 84–89.
93 Z. Ding, S. A. Bligh, L. Tao, J. Quan, H. Nie, L. Zhu and X. Gong, *Mater. Sci. Eng., C*, 2015, **48**, 469–479.
94 T. Guo, Q. Deng, G. Fang, C. Liu, X. Huang and S. Wang, *Biosens. Bioelectron.*, 2015, **74**, 498–503.
95 T. Guo, Q. Deng, G. Fang, D. Gu, Y. Yang and S. Wang, *Biosens. Bioelectron.*, 2016, **79**, 341–346.
96 J. Li, M. Ma, C. Zhang, R. Lu, L. Zhang and W. Zhang, *Anal. Bioanal. Chem.*, 2020, **412**, 7227–7236.
97 L. Qian, W. Liu, H. Liu, V. Nica, S. Zhang, Q. Zhou, W. Song and Q. Zhang, *ACS Appl. Mater. Interfaces*, 2021, **13**, 31010–31020.
98 A. Rachkov and N. Minoura, *Biochem. Biophys. Acta*, 2001, **1544**, 255–266.
99 S. P. Teixeira, R. L. Reis, N. A. Peppas, M. E. Gomes and R. M. Domingues, *Sci. Adv.*, 2021, **7**, eabi9884.
100 S. Dietl, H. Sobek and B. Mizaikoff, *TrAC, Trends Anal. Chem.*, 2021, **143**, 116414.
101 H. Nishino, C. S. Huang and K. J. Shea, *Angew. Chem., Int. Ed.*, 2006, **118**, 2452–2456.
102 K. Yang, J. Liu, S. Li, Q. Li, Q. Wu, Y. Zhou, Q. Zhao, N. Deng, Z. Liang, L. Zhang and Y. Zhang, *Chem. Commun.*, 2014, **50**, 9521–9524.
103 K. Yang, S. Li, J. Liu, L. Liu, L. Zhang and Y. Zhang, *Anal. Chem.*, 2016, **88**, 5621–5625.
104 X. L. Zhao, D. Y. Li, X. W. He, W. Y. Li and Y. K. Zhang, *J. Mater. Chem. B*, 2014, **2**, 7575–7582.
105 S. Li, K. Yang, J. Liu, B. Jiang, L. Zhang and Y. Zhang, *Anal. Chem.*, 2015, **87**, 4617–4620.
106 S. Li, K. Yang, B. Zhao, X. Li, L. Liu, Y. Chen, L. Zhang and Y. Zhang, *J. Mater. Chem. B*, 2016, **4**, 1960–1967.
107 Y. P. Qin, D. Y. Li, X. W. He, W. Y. Li and Y. K. Zhang, *ACS Appl. Mater. Interfaces*, 2016, **8**, 10155–10163.
108 D. Y. Li, X. M. Zhang, Y. J. Yan, X. W. He, W. Y. Li and Y. K. Zhang, *Biosens. Bioelectron.*, 2016, **79**, 187–192.
109 R. Xing, S. Wang, Z. Bie, H. He and Z. Liu, *Nat. Protoc.*, 2017, **12**, 964–987.
110 D. Li, Y. Chen and Z. Liu, *Chem. Soc. Rev.*, 2015, **44**, 8097–8123.
111 Z. Lin, J. Wang, X. Tan, L. Sun, R. Yu, H. Yang and G. Chen, *J. Chromatogr. A*, 2013, **1319**, 141–147.
112 Z. Lin, L. Sun, W. Liu, Z. Xia, H. Yang and G. Chen, *J. Mater. Chem. B*, 2014, **2**, 637–643.
113 L. Sun, D. Lin, G. Lin, L. Wang and Z. Lin, *Anal. Methods*, 2015, **7**, 10026–10031.
114 J. Luo, J. Huang, J. Cong, W. Wei and X. Liu, *ACS Appl. Mater. Interfaces*, 2017, **9**, 7735–7744.
115 X. Y. Sun, R. T. Ma, J. Chen and Y. P. Shi, *Microchim. Acta*, 2017, **184**, 3729–3737.
116 L. Li, Y. Lu, Z. Bie, H. Y. Chen and Z. Liu, *Angew. Chem., Int. Ed.*, 2013, **52**, 7451–7454.
117 S. Wang, J. Ye, Z. Bie and Z. Liu, *Chem. Sci.*, 2014, **5**, 1135–1140.
118 R. R. Xing, Y. Ma, Y. Wang, Y. Wen and Z. Liu, *Chem. Sci.*, 2019, **10**, 1831–1835.
119 R. R. Xing, Z. C. Guo, H. F. Lu, Q. Zhang and Z. Liu, *Sci. Bull.*, 2022, **67**, 278–287.
120 A. Poma, A. Guerreiro, M. J. Whitcombe, E. V. Piletska, A. P. F. Turner and S. A. Piletsky, *Adv. Funct. Mater.*, 2013, **23**, 2821–2827.
121 F. Canfarotta, A. Poma, A. Guerreiro and S. Piletsky, *Nat. Protoc.*, 2016, **11**, 443–455.
122 A. Poma, A. Guerreiro, S. Caygill, E. Moczko and S. Piletsky, *RSC Adv.*, 2014, **4**, 4203–4206.
123 S. Ambrosini, S. Beyazit, K. Haupt and B. Tse Sum Bui, *Chem. Commun.*, 2013, **49**, 6746–6748.
124 J. Xu, K. Haupt and B. Tse Sum Bui, *ACS Appl. Mater. Interfaces*, 2017, **9**, 24476–24483.
125 J. J. Xu, S. Ambrosini, E. Tamahkar, C. Rossi, K. Haupt and B. Tse Sum Bui, *Biomacromolecules*, 2016, **17**, 345–353.
126 J. J. Xu, F. Merlier, B. Avalle, V. Vieilard, P. Debre, K. Haupt and B. T. S. Bui, *ACS Appl. Mater. Interfaces*, 2019, **11**, 9824–9831.
127 J. Ashley, X. Feng, A. Halder, T. Zhou and Y. Sun, *Chem. Commun.*, 2018, **54**, 3355–3358.
128 R. Mahajan, M. Rouhi, S. Shinde, T. Bedwell, A. Incel, L. Mavliutova, S. Piletsky, I. A. Nicholls and B. Sellergren, *Angew. Chem., Int. Ed.*, 2019, **58**, 727–730.
129 A. Cecchini, V. Raffa, F. Canfarotta, G. Signore, S. Piletsky, M. P. MacDonald and A. Cuschieri, *Nano Lett.*, 2017, **17**, 2307–2312.
130 A. Gómez-Caballero, A. Elejaga-Jimeno, G. García del Caño, N. Unceta, A. Guerreiro, M. Saumell-Esnaola, J. Sallés, M. A. Goicolea and R. J. Barrio, *Microchim. Acta*, 2021, **188**, 368.
131 H. Sunayama, T. Ooya and T. Takeuchi, *Biosens. Bioelectron.*, 2010, **26**, 458–462.
132 T. Takeuchi, H. Sunayama, E. Takano and Y. Kitayama, *Adv. Biochem. Eng. Biot.*, 2015, **150**, 95–106.
133 T. Takeuchi and H. Sunayama, *Chem. Commun.*, 2018, **54**, 6243–6251.
134 Y. Suga, H. Sunayama, T. Ooya and T. Takeuchi, *Chem. Commun.*, 2013, **49**, 8450–8452.
135 H. Sunayama, T. Ooya and T. Takeuchi, *Chem. Commun.*, 2014, **50**, 1347–1349.
136 R. Horikawa, H. Sunayama, Y. Kitayama, E. Takano and T. Takeuchi, *Angew. Chem., Int. Ed.*, 2016, **55**, 13023–13027.
137 T. Zhao, J. Wang, J. He, Q. Deng and S. Wang, *Biosens. Bioelectron.*, 2017, **91**, 756–761.
138 T. Morishige, E. Takano, H. Sunayama, Y. Kitayama and T. Takeuchi, *ChemNanoMat*, 2019, **5**, 224–229.
139 X. Wang, S. Yu, J. Wang, J. Yu, M. Arabi, L. Fu, B. Li, J. Li and L. Chen, *Talanta*, 2020, **211**, 120727.
140 J. P. Fan, J. X. Yu, X. M. Yang, X. H. Zhang, T. T. Yuan and H. L. Peng, *Chem. Eng. J.*, 2018, **337**, 722–732.
141 Z. Yang, Y. Zhang, J. Ren, Q. Zhang and B. Zhang, *ACS Appl. Mater. Interfaces*, 2021, **13**, 34829–34842.

142 D. R. K. Weerasuriya, S. Bhakta, K. Hiniduma, C. K. Dixit, M. Shen, Z. Tobin, J. He, S. L. Suib and J. F. Rusling, *ACS Appl. Bio Mater.*, 2021, **4**, 6157–6166.
143 W. Wan, Q. Han, X. Zhang, Y. Xie, J. Sun and M. Ding, *Chem. Commun.*, 2015, **51**, 3541–3544.
144 M. Bertolla, L. Cenci, A. Anesi, E. Ambrosi, F. Tagliaro, L. Vanzetti, G. Guella and A. M. Bossi, *ACS Appl. Mater. Interfaces*, 2017, **9**, 6908–6915.
145 W. Zhang, T. Zhang and Y. Chen, *J. Proteomics*, 2019, **192**, 188–195.
146 X. Bi and Z. Liu, *Anal. Chem.*, 2014, **86**, 959–966.
147 J. Ye, Y. Chen and Z. Liu, *Angew. Chem., Int. Ed.*, 2014, **53**, 10386–10389.
148 S. Patra, E. Roy, R. Madhuri and P. K. Sharma, *Biosens. Bioelectron.*, 2015, **66**, 1–10.
149 V. V. Shumyantseva, T. V. Bulko, L. V. Sigolaeva, A. V. Kuzikov, P. V. Pogodin and A. I. Archakov, *Biosens. Bioelectron.*, 2018, **99**, 216–222.
150 P. Karami, H. Bagheri, M. Johari-Ahar, H. Khoshsafar, F. Arduini and A. Afkhami, *Talanta*, 2019, **202**, 111–122.
151 Y. Liu, S. Fang, J. Zhai and M. Zhao, *Nanoscale*, 2015, **7**, 7162–7167.
152 Y. Zhang, S. Li, X. T. Ma, X. W. He, W. Y. Li and Y. K. Zhang, *Microchim. Acta*, 2020, **187**, 228.
153 Z. C. Guo, R. R. Xing, M. H. Zhao, Y. Li, H. F. Lu and Z. Liu, *Adv. Sci.*, 2021, **8**, 2101713.
154 F. Canfarotta, L. Lezina, A. Guerreiro, J. Czulak, A. Petukhov, A. Daks, K. Smolinska-Kempisty, A. Poma, S. Piletsky and N. A. Barlev, *Nano Lett.*, 2018, **18**, 4641–4646.
155 Y. T. Qin, H. Peng, X. W. He, W. Y. Li and Y. K. Zhang, *Anal. Chem.*, 2019, **91**, 12696–12703.
156 H. Peng, Y. T. Qin, X. W. He, W. Y. Li and Y. K. Zhang, *ACS Appl. Mater. Interfaces*, 2020, **12**, 13360–13370.
157 Y. T. Qin, Y. S. Feng, Y. J. Ma, X. W. He, W. Y. Li and Y. K. Zhang, *ACS Appl. Mater. Interfaces*, 2020, **12**, 24585–24598.
158 H. Y. Wang, P. P. Cao, Z. Y. He, X. W. He, W. Y. Li, Y. H. Li and Y. K. Zhang, *Nanoscale*, 2019, **11**, 17018–17030.
159 C. Jia, M. Zhang, Y. Zhang, Z. B. Ma, N. N. Xiao, X. W. He, W. Y. Li and Y. K. Zhang, *ACS Appl. Mater. Interfaces*, 2019, **11**, 32431–32440.
160 Y. R. Dong, W. Li, Z. K. Gu, R. R. Xing, Y. Y. Ma, Q. Zhang and Z. Liu, *Angew. Chem., Int. Ed.*, 2019, **58**, 10621–10625.
161 Z. K. Gu, Y. R. Dong, S. X. Xu, L. S. Wang and Z. Liu, *Angew. Chem., Int. Ed.*, 2021, **133**, 2695–2699.
162 P. X. M. Rangel, E. Moroni, F. Merlier, L. A. Gheber, R. Vago, B. T. S. Bui and K. Haupt, *Angew. Chem., Int. Ed.*, 2020, **59**, 2816–2822.
163 H. F. Lu, S. X. Xu, Z. C. Guo, M. H. Zhao and Z. Liu, *ACS Nano*, 2021, **15**, 18214–18225.